Spectral Games

Marc Kachelrieß

German Cancer Research Center (DKFZ)
Heidelberg, Germany
www.dkfz.de/ct

dkfz. DEUTSCHES KREBSFORSCHUNGSZENTRUM IN DER HELMHOLTZ-GEMEINSCHAFT

Aim

- You never know the x-ray spectrum of a real system.
- To give some examples of how to cope with this situation.

Detected X-Ray Spectrum

- Of relevance for artifact correction is the detected spectrum *w*(*E*), and not the emitted spectrum *I*(*E*).
- Emitted spectrum, i.e. photon numbers or intensities (involves intrinsic and extrinsic prefiltration):

$$I(E)$$

- Detected spectrum, simple model:

$$w(E) \propto E^{01}\, I(E)\, \left(1 - e^{-\mu_{\mathrm{D}}(E) d_{\mathrm{D}}}\right)$$

Normalization to unit area.

- Spectra are functions of the detector pixel position (*u*, *v*).

$$w(u, v, E) \propto E^{01}\, I(u, v, E)\, \left(1 - e^{-\mu_{\mathrm{D}}(E) d_{\mathrm{D}}(u, v)}\right)$$

Heel Effect

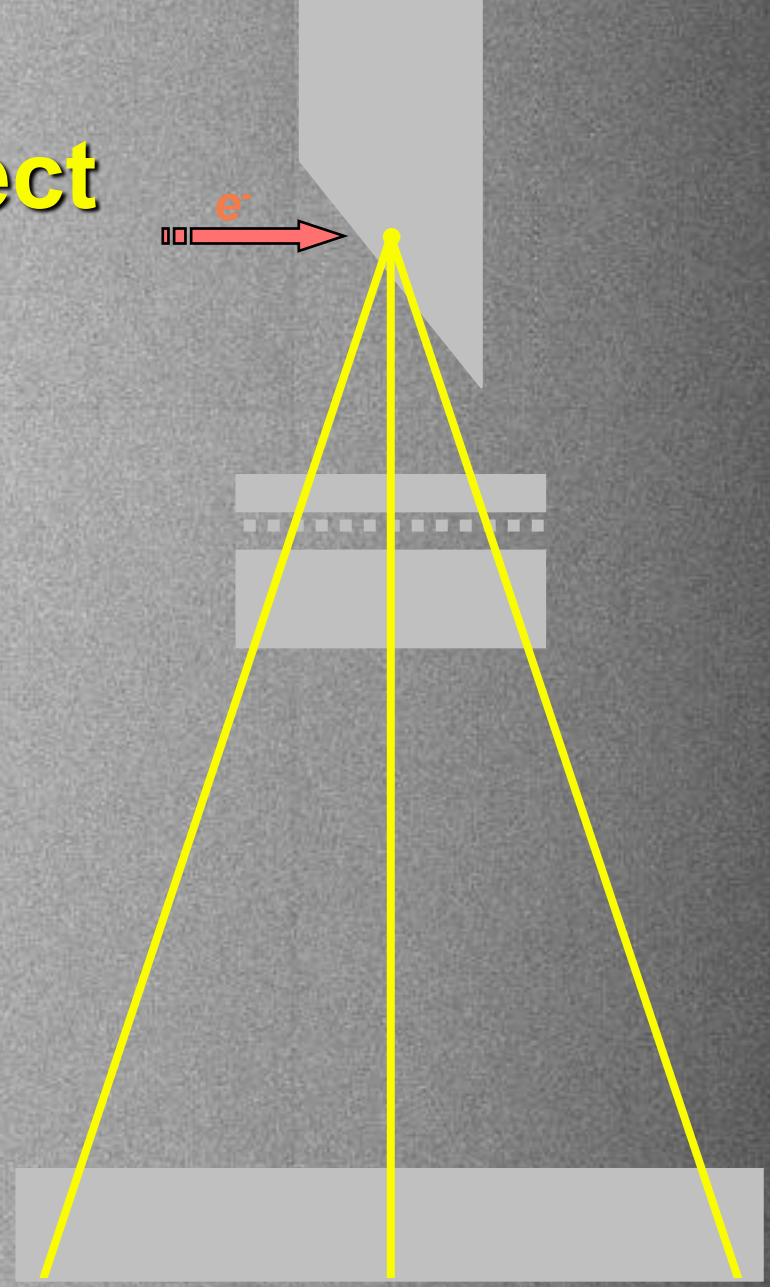

Offset-corrected image (40 kV, 1.39 mA, 23 ms, Ziehm Imaging CMOS)

Simple Spectrum Model

- Assume patient to be decomposed into two materials, pt1 and pt2.
- Observed spectrum (ano = anode, pr = prefilters, bwt = bowtie, pt = patient, det = detector):

$$
\begin{aligned}
w(E) \propto\ & E^{01} N_0(U,E)\, e^{-\mu_{\mathrm{ano}}(E) d_{\mathrm{ano}}(u,v)} \\
& \times e^{-\mu_{\mathrm{pr1}}(E) d_{\mathrm{pr1}}(u,v)} e^{-\mu_{\mathrm{pr2}}(E) d_{\mathrm{pr2}}(u,v)} \\
& \times e^{-\mu_{\mathrm{bwt}}(E) d_{\mathrm{bwt}}(u,v)} \\
& \times e^{-\mu_{\mathrm{pt1}}(E) l_{\mathrm{pt1}}(u,v)} e^{-\mu_{\mathrm{pt2}}(E) l_{\mathrm{pt2}}(u,v)} \\
& \times \left(1 - e^{-\mu_{\mathrm{det}}(E) d_{\mathrm{det}}(u,v)}\right)
\end{aligned}
$$

- Detected spectrum is obtained by setting $l_{\mathrm{pt1}} = l_{\mathrm{pt2}} = 0$.

Estimating the detected spectrum

X-RAY SPECTRUM ESTIMATION

Estimation of the X-Ray Spectrum

- Monte-Carlo simulation of single electron tracks through target[1]
- Target configuration of an industrial CT system

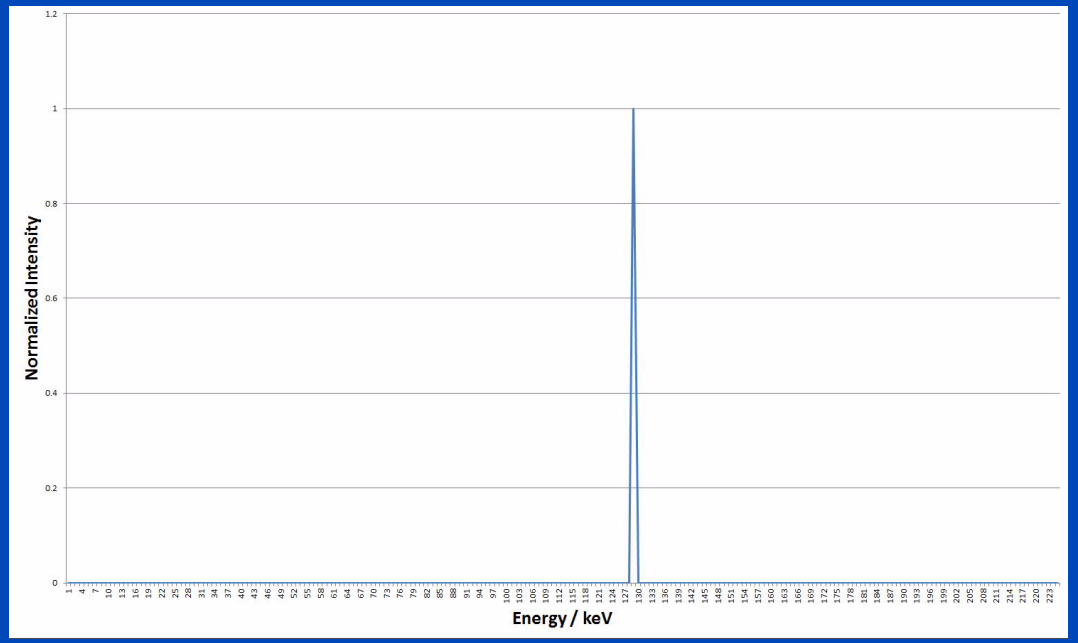

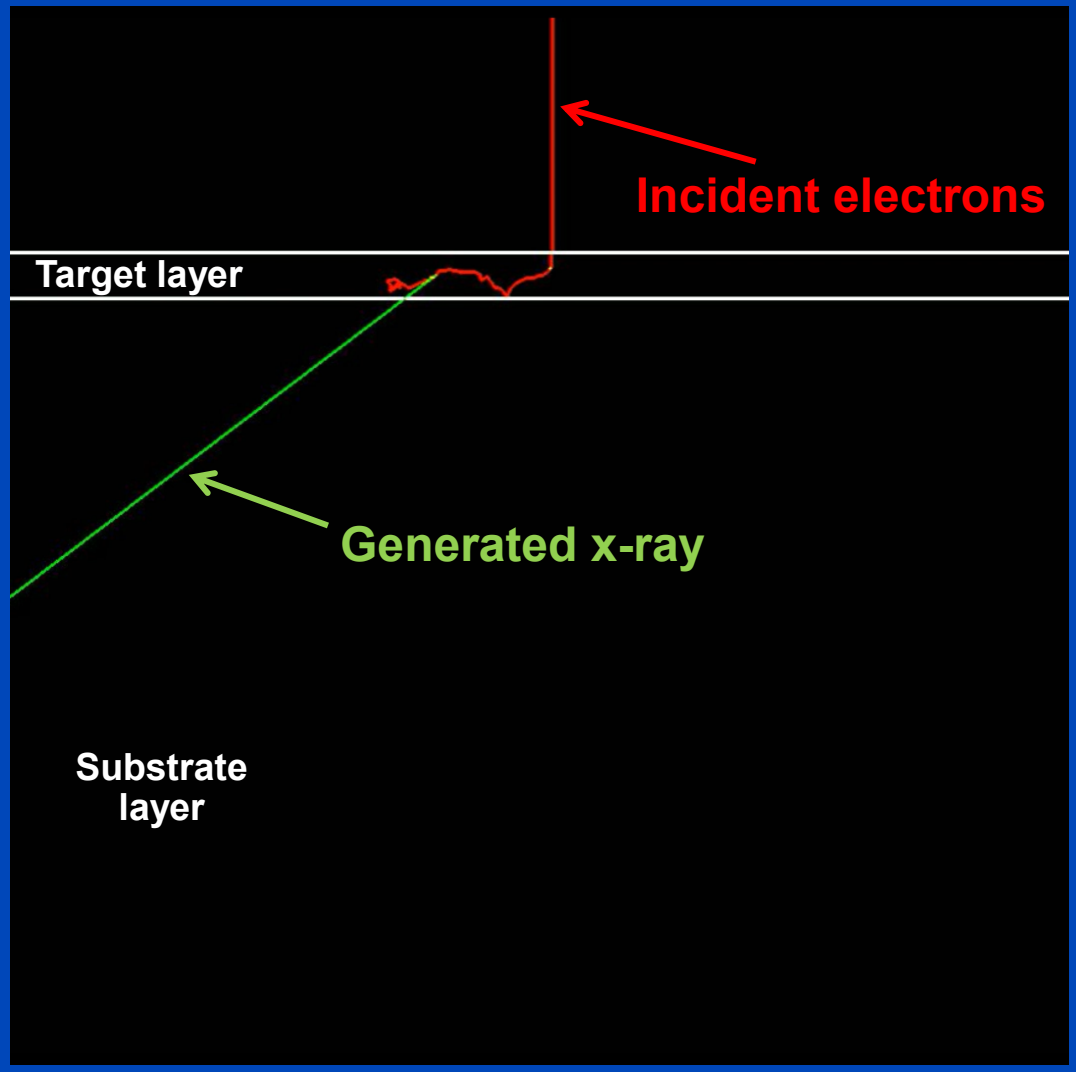

U = 215 kV, 6 µm tungsten target, 250 µm diamond substrate

[1]S. Agostinelli et al, "Geant4—a simulation toolkit", Nucl. Instrum. Meth. A. 506(3), 250-303 (2003)

dkfz.

Introduction

- CT applications that require accurate knowledge of the emitted or detected spectrum:
  - Organ dose estimation
  - Beam hardening correction
  - Dual energy decomposition
  - K-edge imaging
  - Quantitative perfusion measurements
  - …
- Existing methods:
  - Semi-analytic models
  - Monte-Carlo simulation
  - Spectroscopy
  - Compton scattering
  - Transmission measurements (direct, simple, no extra hardware)
  - …

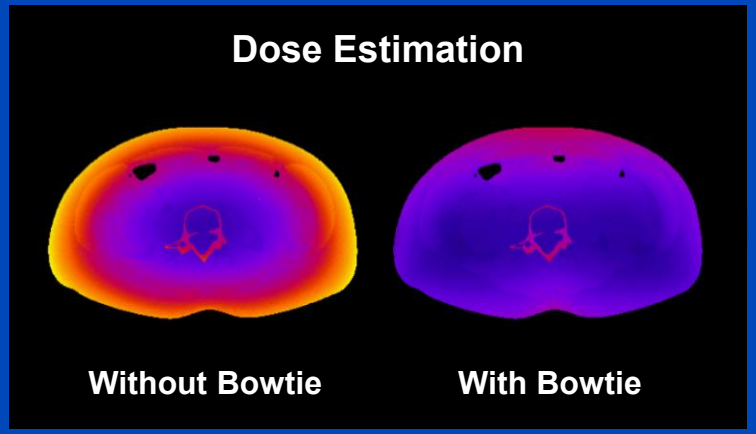

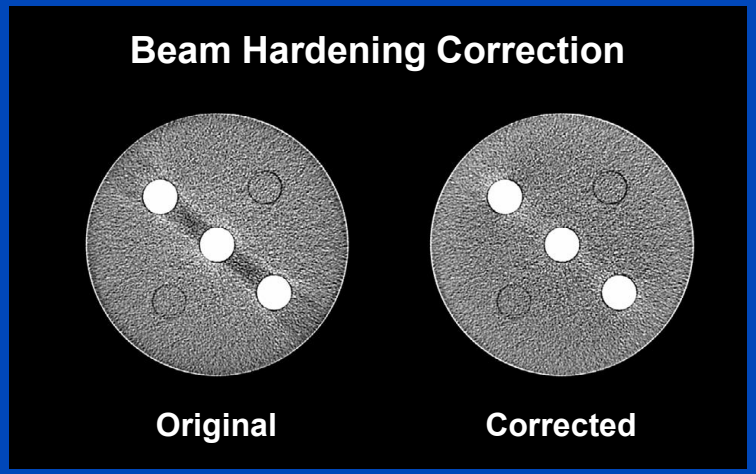

Spectrum Estimation by Attenuation Measurements

X-ray spectrum estimation for accurate attenuation simulation

Carsten Leinweber, Joscha Maier, and Marc Kachelrieß[a)]
German Cancer Research Center (DKFZ), Heidelberg, BW, Germany

(Received 12 January 2017; revised 3 September 2017; accepted for publication 15 September 2017; published 28 October 2017)

Purpose: To estimate detected x-ray spectra from transmission measurements of known attenuators that allow to accurately simulate the transmission in unknown attenuators.
Methods: Starting from the established spectrum estimation method using the truncated singular value decomposition (TSVD) we extended the algorithm by incorporating prior knowledge about the statistical nature of the transmission data and about high-frequency spectral components like characteristic peaks. Thereby our proposed approach requires only minimal prior knowledge, namely the energy positions of characteristic peaks or k-edges, which are typically well-known. This ensures that the final spectrum is not biased towards a given prior spectrum which is often observed in other methods. The new approach, prior truncated singular value decomposition (PTSVD), is compared to TSVD as well as the expectation–maximization (EM) method in a simulation and a measurement study. The resulting spectra are evaluated according to their ability to reproduce transmission data of attenuators that have not been included into the estimation process.
Results: In case of noiseless simulated data, the PTSVD approach outperforms the existing methods in both, estimating the shape of the spectrum as well as providing a spectrum that reproduces the transmission data. Not surprisingly for increasing noise the ability of PTSVD to estimate the spectral shape worsens while it still performs best in reproducing the transmission data. This finding is also confirmed in the measurement study.
Conclusion: Our new approach allows to estimate detected x-ray spectra that accurately reproduce both transmission measurements that have and have not been included into the estimation process. It is less prone to noise compared to the established TSVD method and potentially leads to smaller transmission errors compared to EM for accurate transmission data while being less biased towards the given prior information. [https://doi.org/10.1002/mp.12607]

dkfz.

Spectrum Reconstruction from Transmission Measurements

- **Lambert-Beer law:**

$$\tau_m = \frac{N_m}{N_0} = \sum_{b=1}^{B} e^{-\mu_{mb}\, d_m\, w_b}$$

- **Problem:**

  "Given *τ* for different (known) combinations of *μ*(E) and *d*, reconstruct w(E)."

- **Methods:**
  - **Few parameter modelling**
  - **Neural networks**
  - **Expectation maximization (EM)**
  - **Truncated singular value decomposition (TSVD)**
  - **New: PTSVD**

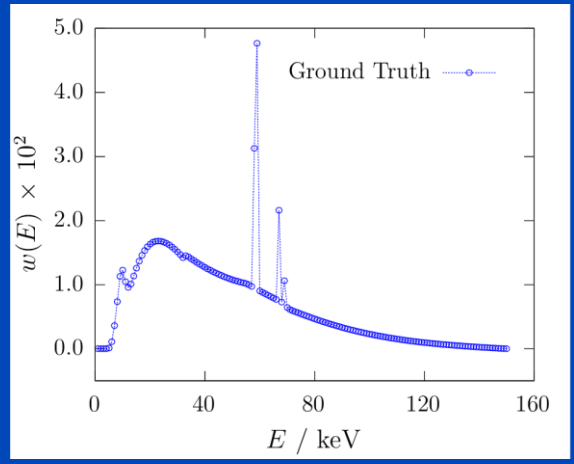

Materials and Methods

Truncated Singular Value Decomposition (TSVD)

- Discretized Lambert-Beer law in matrix notation:

$$\tau_m = \sum_{b=1}^{B} a_{mb}\, w_b \longrightarrow \boldsymbol{\tau} = \boldsymbol{A} \cdot \boldsymbol{w}$$

- Minimize the least square difference

$$\boldsymbol{w} = \arg\min_{\boldsymbol{w}} \|\boldsymbol{A} \cdot \boldsymbol{w} - \boldsymbol{\tau}\|_2^2 \longrightarrow \boldsymbol{w} = \boldsymbol{A}^{+} \cdot \boldsymbol{\tau}$$

- Calculation of the pseudo-inverse A^+
  - Decompose A into orthonormal basis with help of SVD:

$$\boldsymbol{A} = \sum_{b=1}^{B} \boldsymbol{u}_b \cdot s_b \boldsymbol{v}_b^T$$

  - Truncate A^+ to the highest R singular values:

$$\boldsymbol{w} = \sum_{b=1}^{R} \left(\boldsymbol{v}_b \cdot \frac{\boldsymbol{u}_b^T}{s_b} \right) \cdot \boldsymbol{\tau} \qquad R \leq B$$

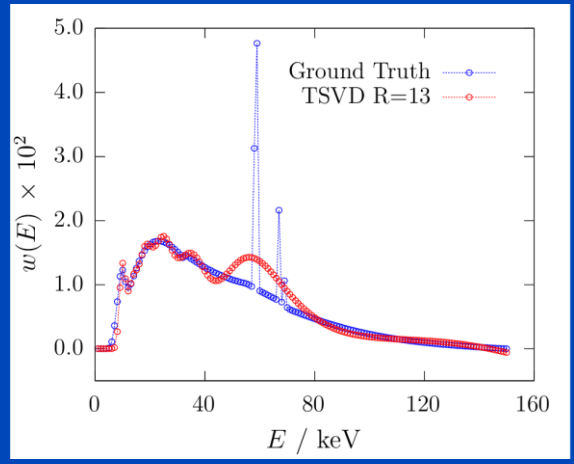

Materials and Methods

Prior Truncated Singular Value Decomposition (PTSVD)

- Minimize the weighted least square difference with help of TSVD to obtain the low frequent solution from range:

$$\boldsymbol{w}_R = \arg\min_{\boldsymbol{w}} \|\boldsymbol{A}\cdot\boldsymbol{w}-\boldsymbol{\tau}\|_W^2 \quad \text{with} \quad \boldsymbol{W} = \mathrm{Cov}(\boldsymbol{\tau},\boldsymbol{\tau})^{-1}$$

- Calculate a solution from null space that represents the high frequency components (here: characteristic peaks):

$$\boldsymbol{w}_\mathrm{N} = \sum_{b=R+1}^{B} \left(\boldsymbol{v}_b^T \cdot \boldsymbol{w}_\mathrm{H}\right) \boldsymbol{v}_b$$

- Add the solution from null space to the solution from range:

$$\boldsymbol{w} = \boldsymbol{w}_R + \boldsymbol{w}_N$$

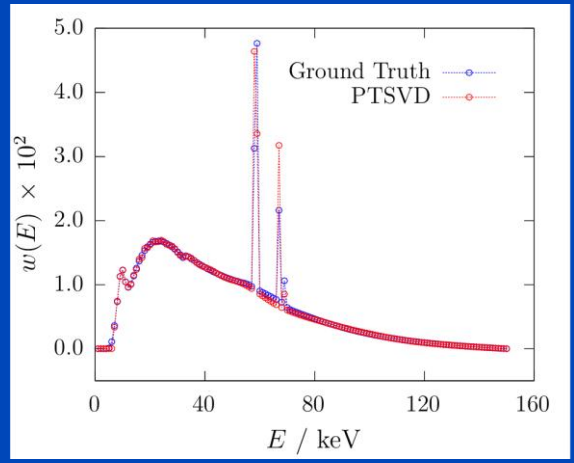

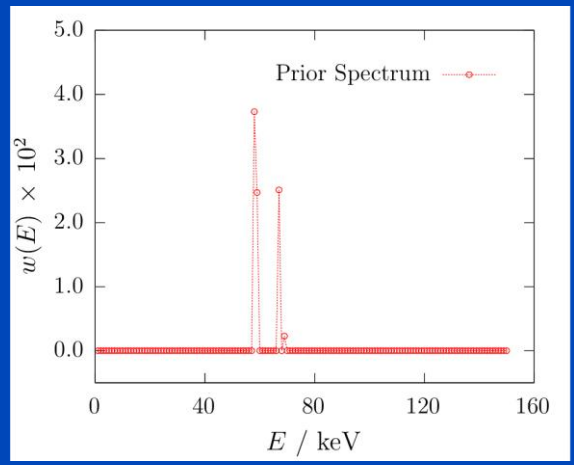

dkfz.

Materials and Methods
Simulation / Measurement Study

- **Simulation conditions:**
  - 150 kV tungsten target spectrum simulated according to Tucker et al.
  - Spectrum estimation from 28 aluminum (Al) attenuators with lengths ranging from 0.5 mm to 132.5 mm
  - Poisson noise is added to the Al transmission data for varying numbers N_0 of incident photons
  - Noiseless simulations of polyoxymethylene (POM) with continuous attenuation length for validation
- **Measurement conditions:**
  - Experimental setup consisting of a 150 kV transmission x-ray tube and a flat detector
  - 28 measurements of Al and POM attenuators with attenuation lengths ranging from 0.5 mm to 132.5 mm
  - Material for spectrum estimation: Al
  - Material for spectrum validation: POM

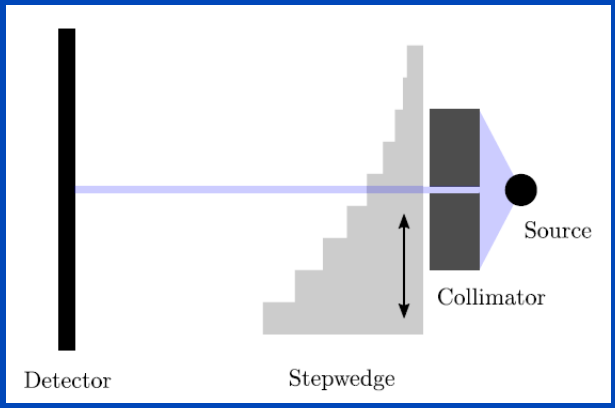

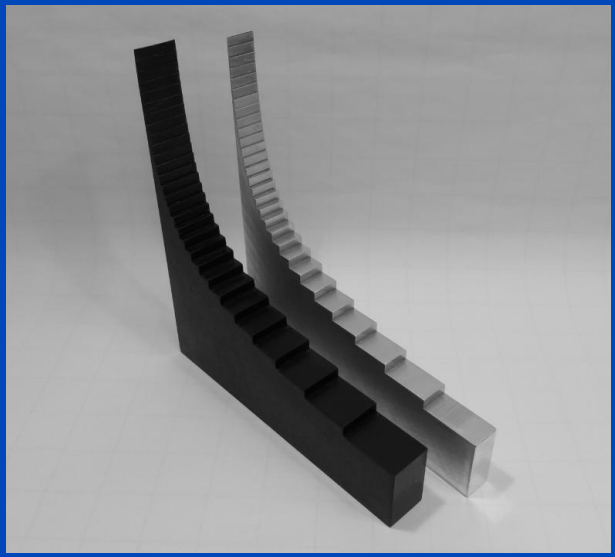

Tucker et al. - Semi-empirical Model for Generating Tungsten Target X-ray Spectra (1989)

dkfz.

Results:
Noiseless Simulated Data

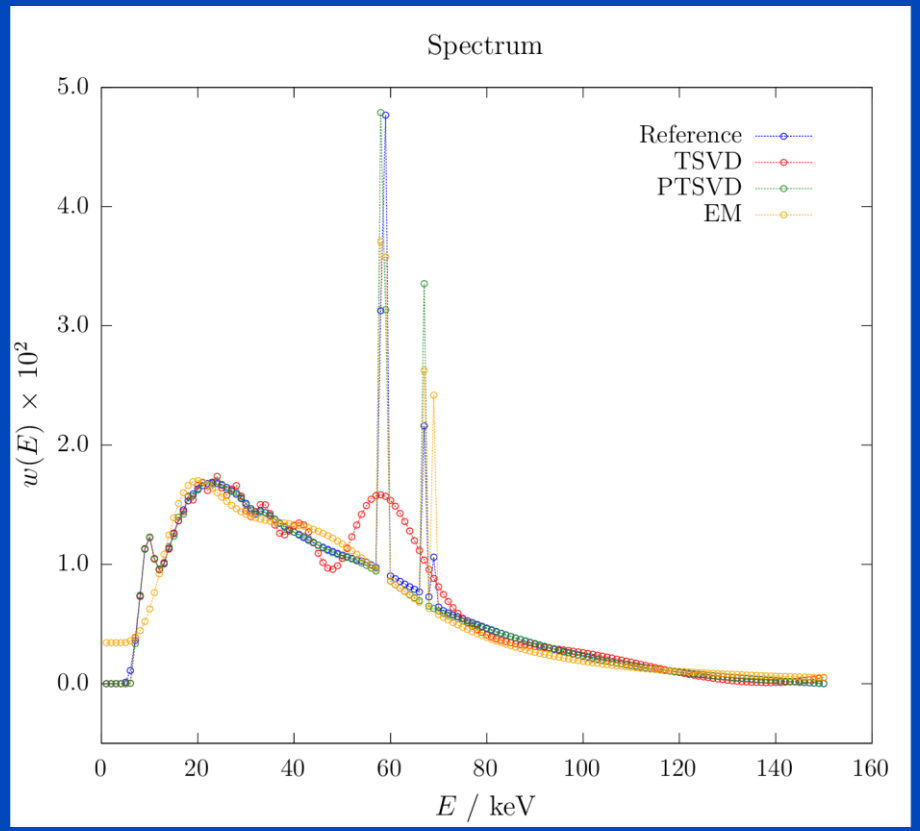

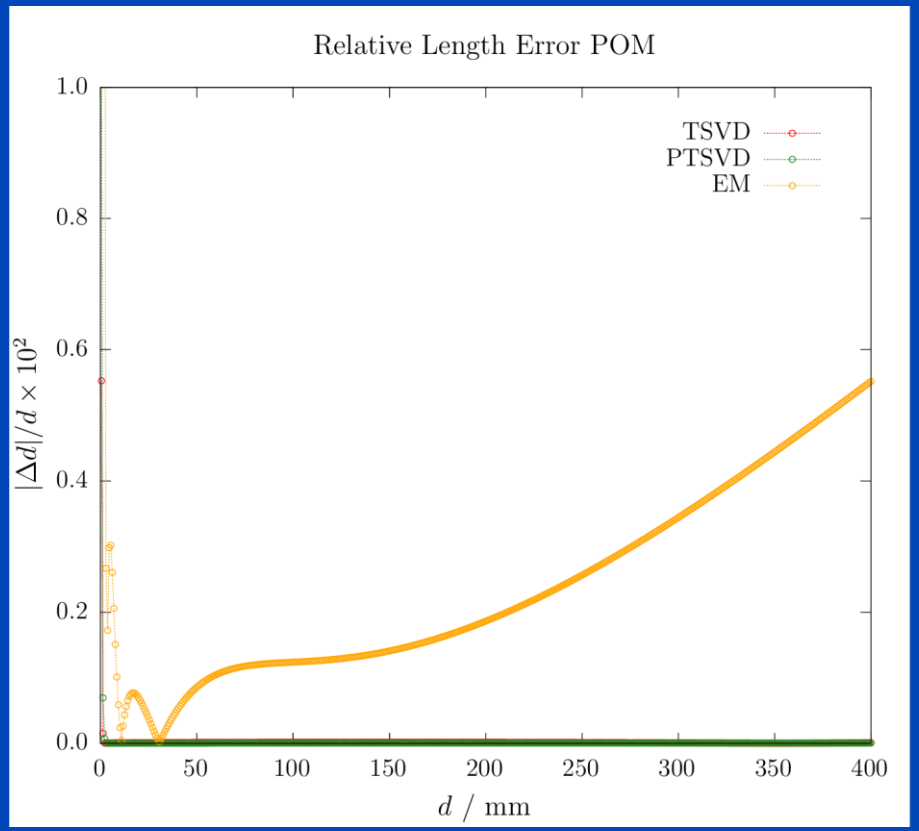

$$\frac{|\Delta d|}{d} = \frac{|d' - d|}{d}$$

Results

Noisy Simulated Data
$N_0 = 1 \times 10^{12}$

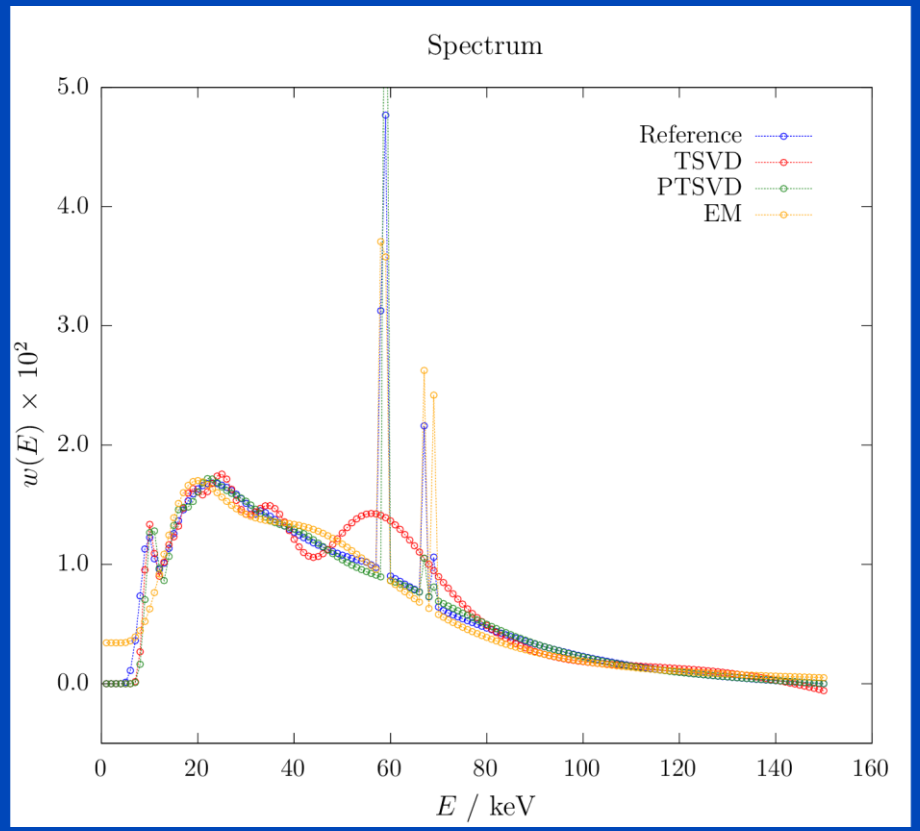

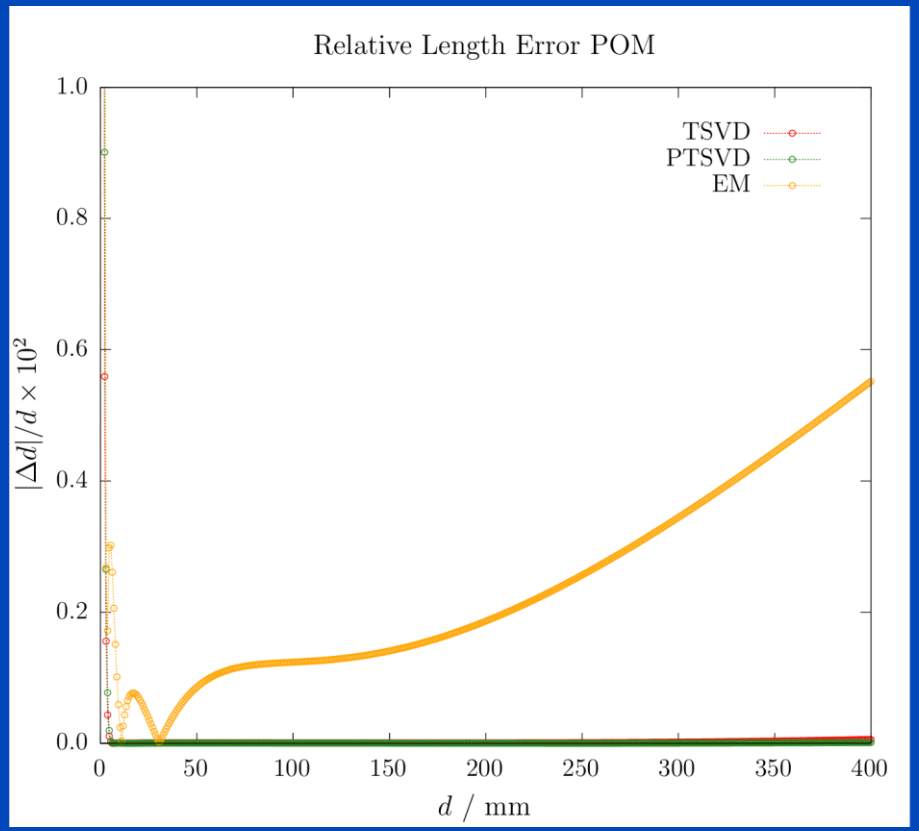

$$\frac{|\Delta d|}{d} = \frac{|d' - d|}{d}$$

Results

Noisy Simulated Data
$N_0 = 1 \times 10^{10}$

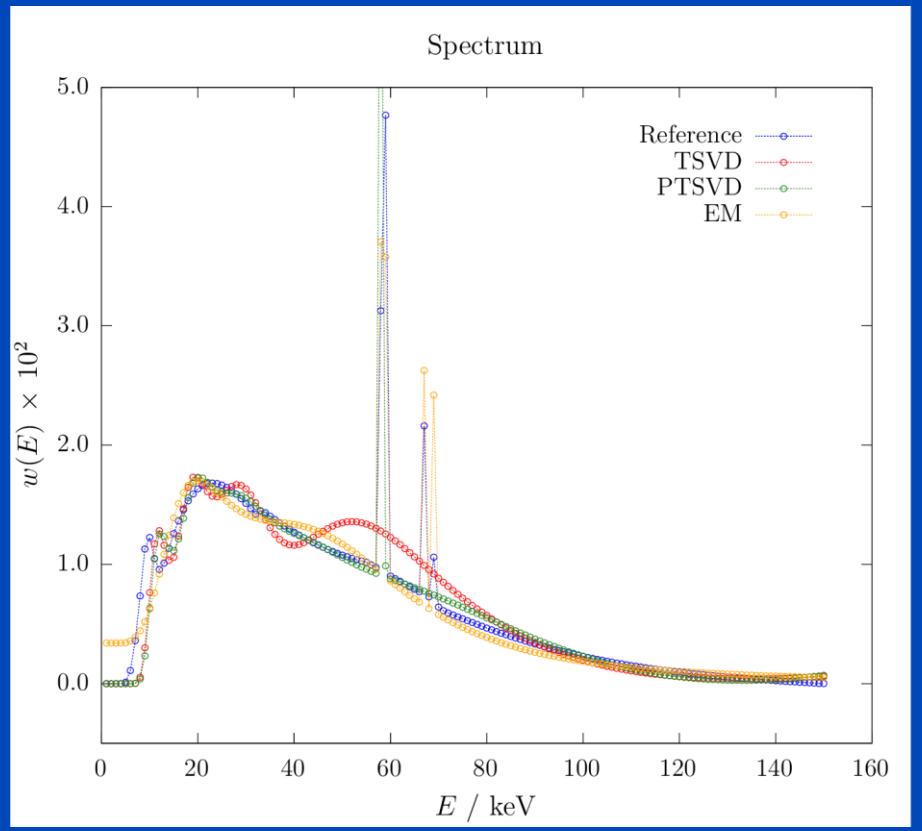

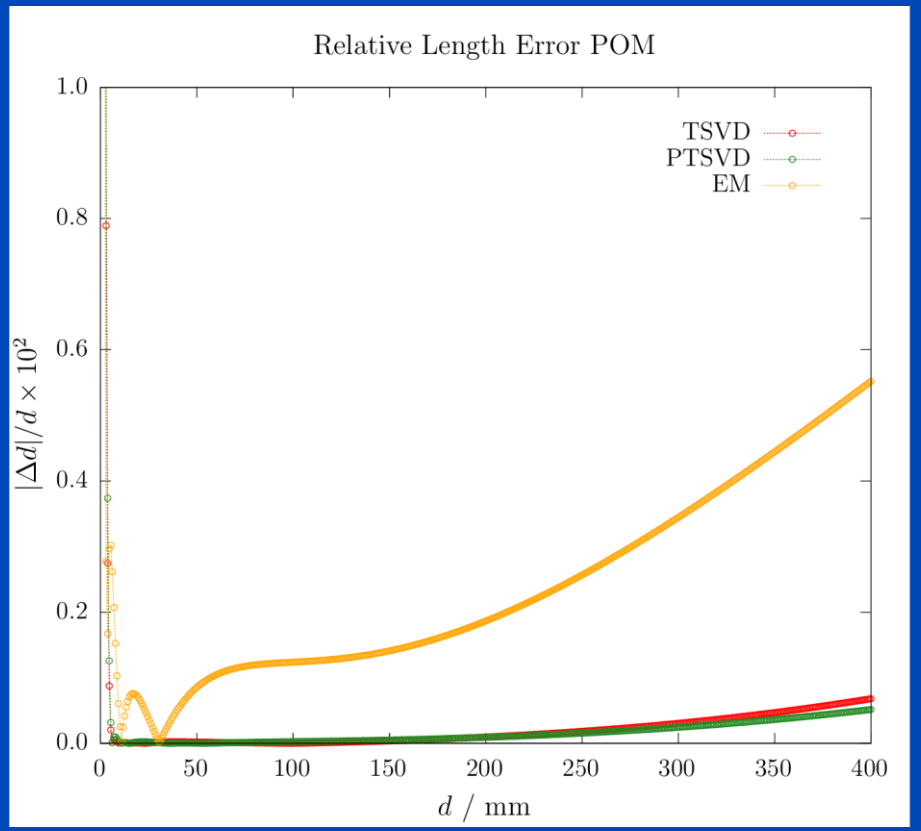

$$\frac{|\Delta d|}{d} = \frac{|d' - d|}{d}$$

Results

Noisy Simulated Data
$N_0 = 1 \times 10^8$

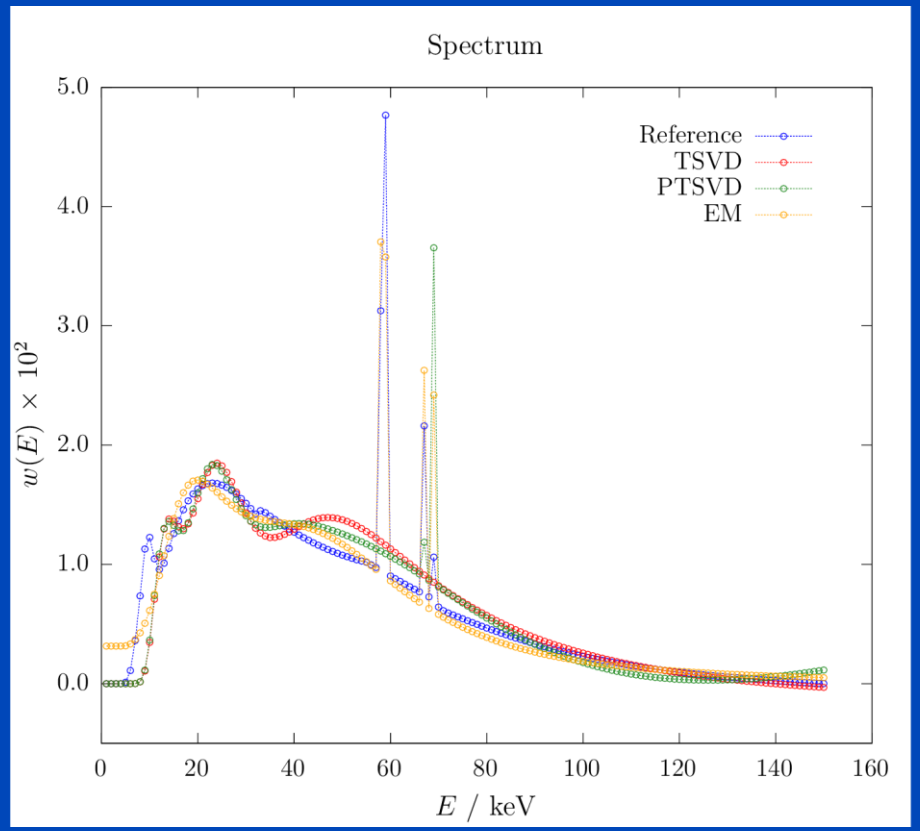

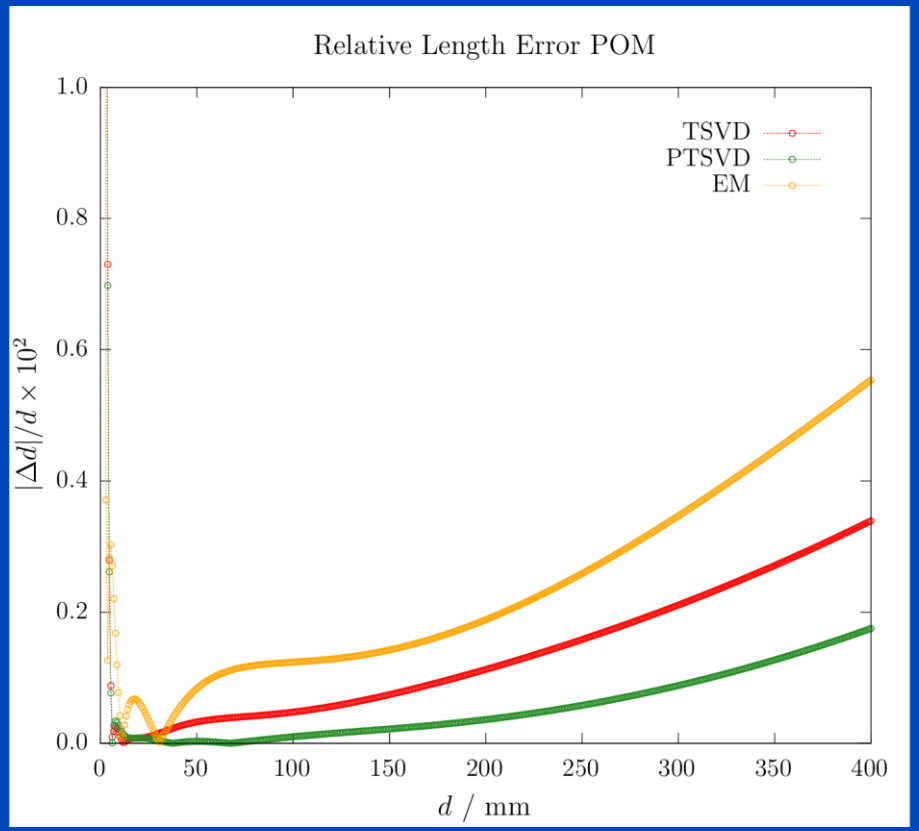

$$\frac{|\Delta d|}{d} = \frac{|d' - d|}{d}$$

Results

Noisy Simulated Data
$N_0 = 1 \times 10^6$

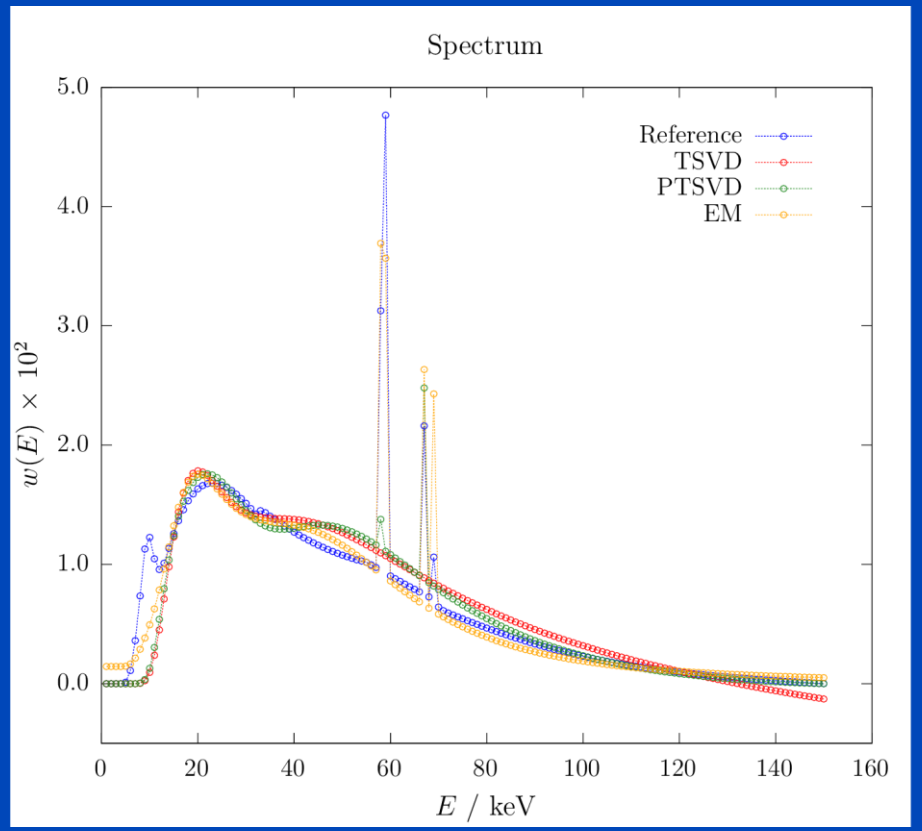

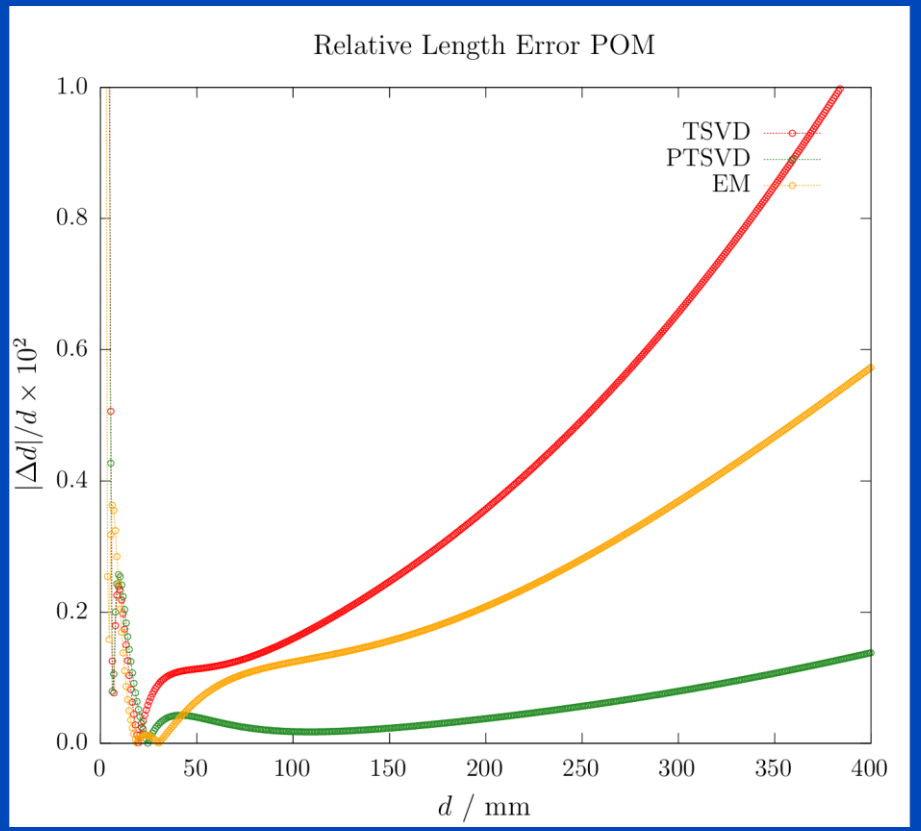

$$\frac{|\Delta d|}{d} = \frac{|d' - d|}{d}$$

dkfz.

Results

Measured Data

$N_0 \approx 1 \times 10^{10}$

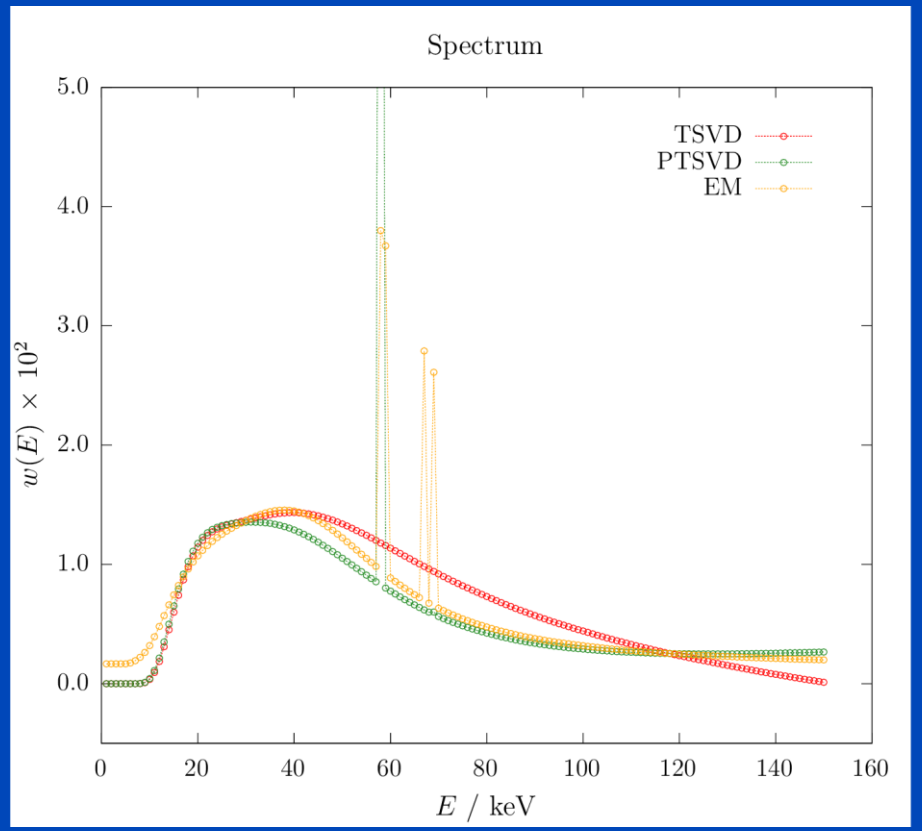

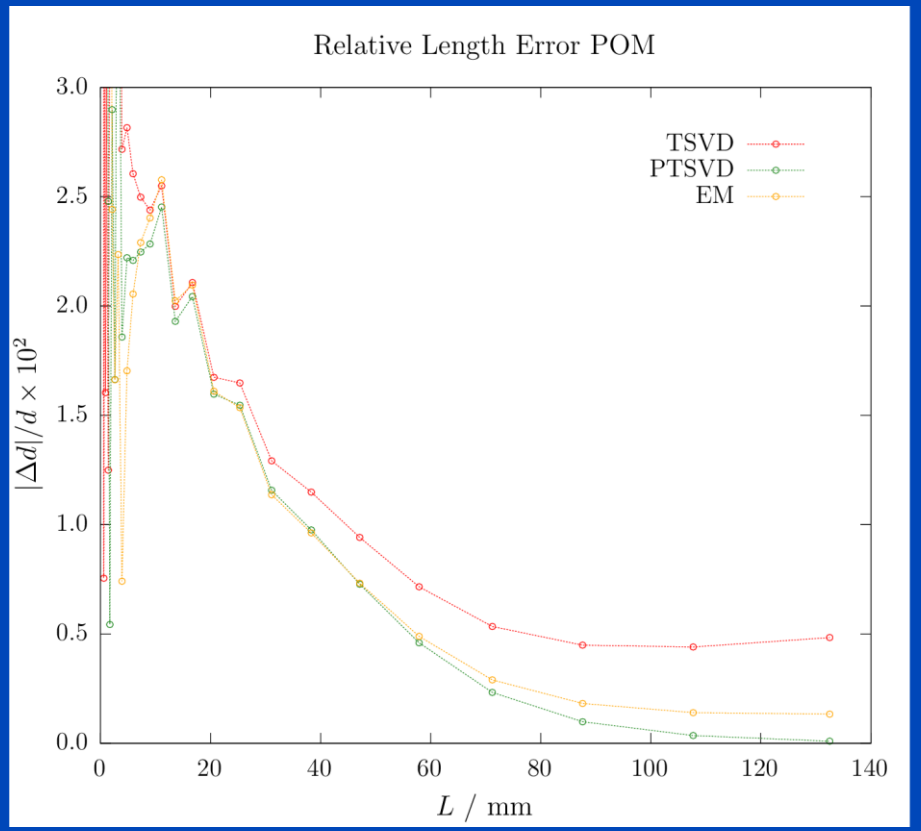

$$\frac{|\Delta d|}{d} = \frac{|d' - d|}{d}$$

Conclusion and Discussion

- PTSVD overcomes the limitations of TSVD by incorporating prior information about the statistical nature of the transmission data and about the high frequency components of the spectrum.
- PTSVD is less prone to noise compared to TSVD.
- Simulations show that for accurate transmission data PTSVD leads to smaller length errors compared to EM.
- Effects that limit the accuracy of transmission measurements: quantum noise, electronic noise, scattered radiation, image lag, quantization errors, dynamic range, …

FIRST ORDER
BEAM HARDENING CORRECTION

Beam Hardening

- **Measurement**

$$q = -\ln \int dE\, w(E) e^{-\int dL\, \mu(\boldsymbol{r}, E)}$$

- **Single material approximation:** $\mu(\boldsymbol{r}, E) = f_1(\boldsymbol{r})\psi_1(E)$

$$q = -\ln \int dE\, w(E) e^{-p_1 \psi_1(E)}$$

→ cupping, first order BH artifacts → cupping correction (water precorrection)

- **Two material case:** $\mu(\boldsymbol{r}, E) = f_1(\boldsymbol{r})\psi_1(E) + f_2(\boldsymbol{r})\psi_2(E)$

$$q = -\ln \int dE\, w(E) e^{-p_1 \psi_1(E) - p_2 \psi_2(E)}$$

→ banding artifacts, higher order BH artifacts → higher order BH correction

First Order Beam Hardening

32 cm Water Phantom

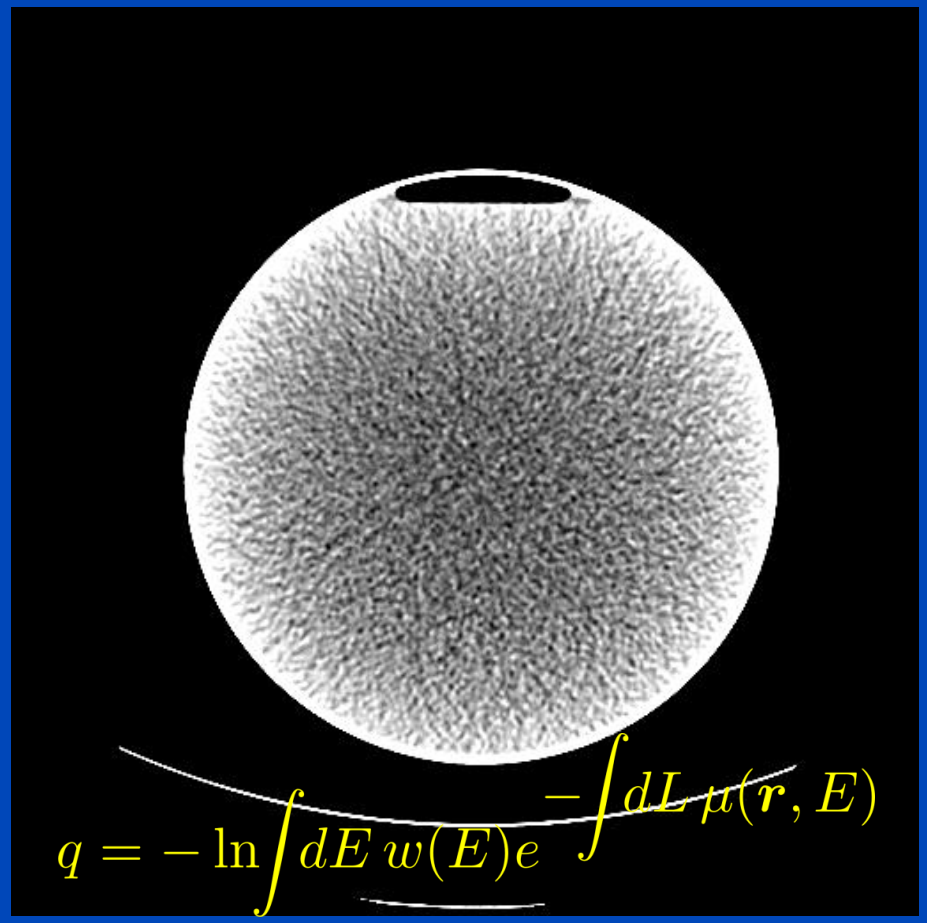

Phantom with Water Precorrection

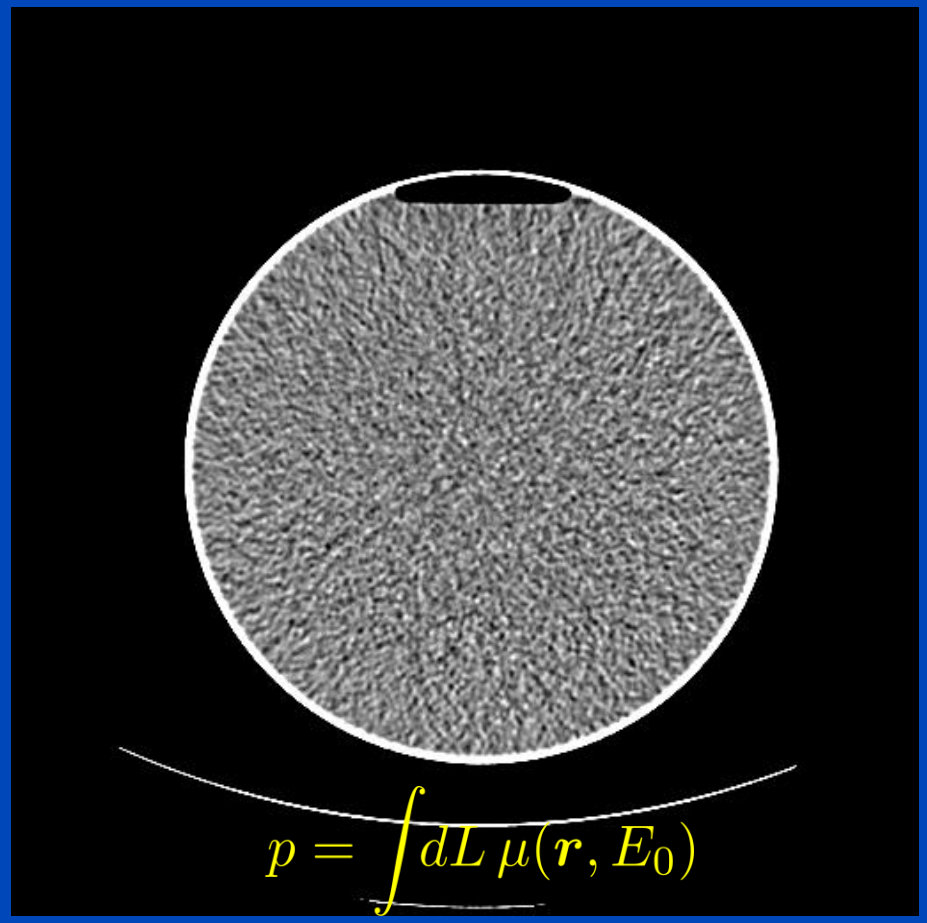

Water Precorrection: Determine a function *P* such that *p* = *P*(*q*) corrects for the cupping.

C = 0 HU, *W* = 100 HU

dkfz.

Analytical Cupping Correction

- **Know the detected spectrum, e.g.**

$$w(E) \propto E\, I(E)\left(1 - e^{-\mu_{\mathrm{D}}(E) d_{\mathrm{D}}}\right)$$

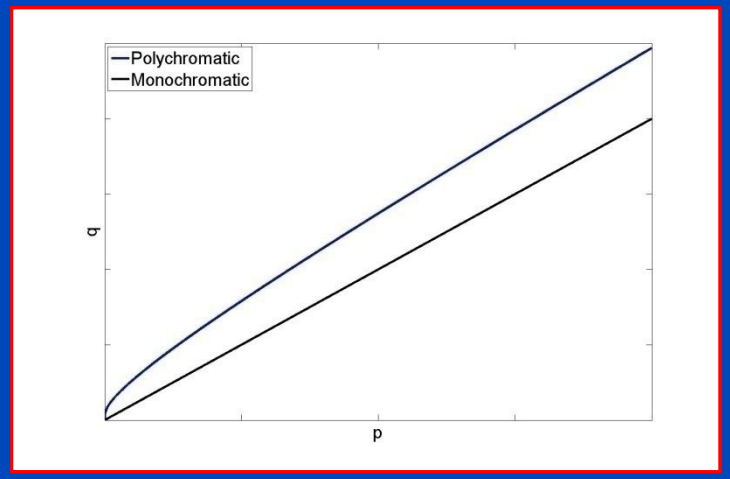

- **Assume the object to be decomposed as**

$$\mu(\boldsymbol{r}, E) = f(\boldsymbol{r})\psi(E)$$

such that

$$q = -\ln \int dE\, w(E) e^{-p\,\psi(E)} \quad \textbf{with} \quad p = \int dL\, f(\boldsymbol{r})$$

- **Invert (numerically) to get**

$$p = P(q)$$

Works iff you know *w*(*E*) and *ψ*(*E*).

Alternatives if Spectra are Unknown

- Calibrate water precorrection function.
  - Use layers of known thickness d_n, e.g. PE sheets in steps of 10 mm.
  - This yields a LUT $q(d)$ that can be inverted.
  - This can be done pixel-wise and thus account for the heel effect and others.

Empirical cupping correction: A first-order raw data precorrection for cone-beam computed tomography

Marc Kachelrieß,[a] Katia Sourbelle, and Willi A. Kalender
Institute of Medical Physics, University of Erlangen-Nürnberg, Henkestraße 91, D-91052 Erlangen Germany

(Received 5 December 2005; revised 13 February 2006; accepted for publication 21 February 2006; published 19 April 2006)

We propose an empirical cupping correction (ECC) algorithm to correct for CT cupping artifacts that are induced by nonlinearities in the projection data. The method is raw and requires neither knowledge of the x-ray spectrum nor of the attenuation linearizing the attenuation data using a precorrection function of polynomia of the polynomial are determined once using a calibration scan of a homog puting the coefficients is done in image domain by fitting a series of basi image. The template image is obtained directly from the uncorrected phar sumptions on the phantom size or of its positioning are made. Raw data are them through the once-determined polynomial. As an example we demons used to perform water precorrection for an *in vivo* micro-CT scanner (To GmbH, Erlangen, Germany). For this particular case, practical considerati tion of the template image are given. ECC strives to remove the cupping well-calibrated CT values. Although ECC is a first-order correction and iterative higher-order beam hardening or scatter correction algorithms, our show a significant reduction of bone-induced artifacts as well. A combinatio cal techniques yielding a hybrid cupping correction method is possible a dependent correction functions. © *2006 American Association of Phy*
[DOI: 10.1118/1.2188076]

Key words: flat-panel detector CT, C-arm CT, micro-CT, artifacts, image

I. INTRODUCTION

Due to beam polychromacity in CT, the energy dependence of the attenuation coefficients, and scatter, the log-

know the calibrati
Therefore, it has si
ing approaches that
ECC aims at lin

Empirical dual energy calibration (EDEC) for cone-beam computed tomography

Philip Stenner, Timo Berkus, and Marc Kachelriess
Institute of Medical Physics, University of Erlangen-Nürnberg, Henkestrasse 91, Erlangen, 91052 Germany

(Received 1 February 2007; revised 25 June 2007; accepted for publication 17 July 2007; published 24 August 2007)

Material-selective imaging using dual energy CT (DECT) relies heavily on well-calibrated material decomposition functions. These require the precise knowledge of the detected x-ray spectra, and even if they are exactly known the reliability of DECT will suffer from scattered radiation. We propose an empirical method to determine the proper decomposition function. In contrast to other decomposition algorithms our empirical dual energy calibration (EDEC) technique requires neither knowledge of the spectra nor of the attenuation coefficients. The desired material-selective raw data p_1 and p_2 are obtained as functions of the measured attenuation data q_1 and q_2 (one DECT scan =two raw data sets) by passing them through a polynomial function. The polynomial's coefficients are determined using a general least squares fit based on thresholded images of a calibration phantom. The calibration phantom's dimension should be of the same order of magnitude as the test object, but other than that no assumptions on its exact size or positioning are made. Once the decomposition coefficients are determined DECT raw data can be decomposed by simply passing them through the polynomial. To demonstrate EDEC simulations of an oval CTDI phantom, a lung phantom, a thorax phantom and a mouse phantom were carried out. The method was further verified by measuring a physical mouse phantom, a half-and-half-cylinder phantom and a Yin-Yang phantom with a dedicated *in vivo* dual source micro-CT scanner. The raw data were decomposed into their components, reconstructed, and the pixel values obtained were compared to the theoretical values. The determination of the calibration coefficients with EDEC is very robust and depends only slightly on the type of calibration phantom used. The images of the test phantoms (simulations and measurements) show a nearly perfect agreement with the theoretical μ values and density values. Since EDEC is an empirical technique it inherently compensates for scatter components. The empirical dual energy calibration technique is a pragmatic, simple, and reliable calibration approach that produces highly quantitative DECT images. © *2007 American Association of Physicists in Medicine*. [DOI: 10.1118/1.2769104]

M. Kachelrieß, K. Sourbelle, and W.A. Kalender, "Empirical cupping correction: A first-order raw data precorrection for cone-beam computed tomography," Med. Phys. 33(5):1269-1274, May 2006.

dkfz.

Empirical Cupping Correction (ECC)

- Series expansion of the precorrection function

$$p = P(q) = \sum_n c_n P_n(q) = \sum_n c_n q^n$$

- Go to image domain by reconstructing q^n

$$f_n(\boldsymbol{r}) = \mathsf{X}^{-1} P_n(q) = \mathsf{X}^{-1} q^n$$

- Find coefficients from

$$f(\boldsymbol{r}) = \mathsf{X}^{-1} p = \mathsf{X}^{-1} P(q) = \sum_n c_n f_n(\boldsymbol{r})$$

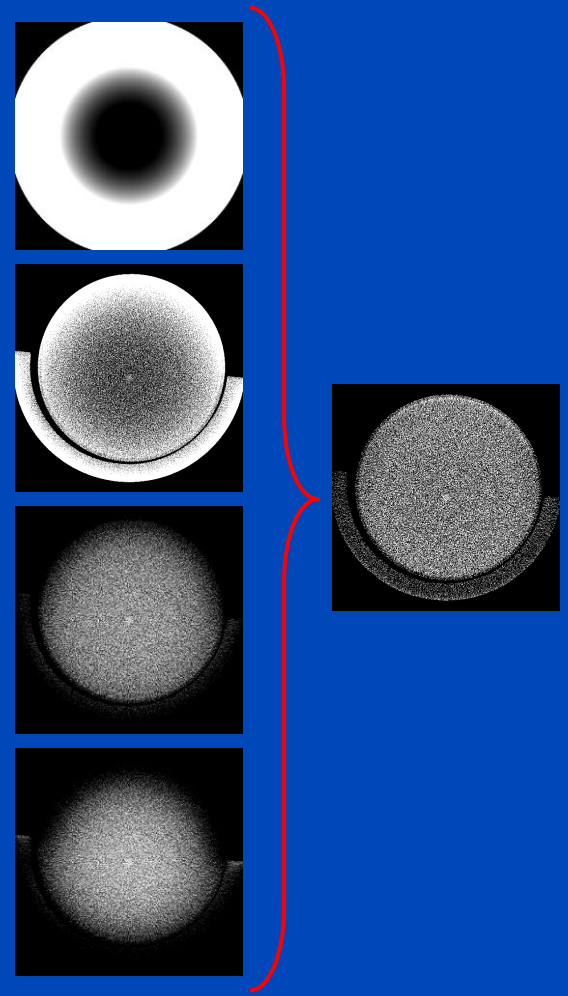

M. Kachelrieß, K. Sourbelle, and W.A. Kalender, "Empirical cupping correction: A first-order raw data precorrection for cone-beam computed tomography," Med. Phys. 33(5):1269-1274, May 2006.

ECC Template Image

$$\boldsymbol{c} = \arg\min_{\boldsymbol{c}} \int d^3r\, w(\boldsymbol{r})\big(f(\boldsymbol{r}) - t(\boldsymbol{r})\big)^2$$

$$f(\boldsymbol{r}) = \sum_n c_n f_n(\boldsymbol{r})$$

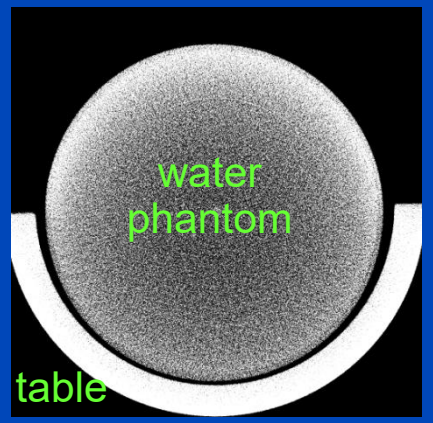

segment and
specify CT-values

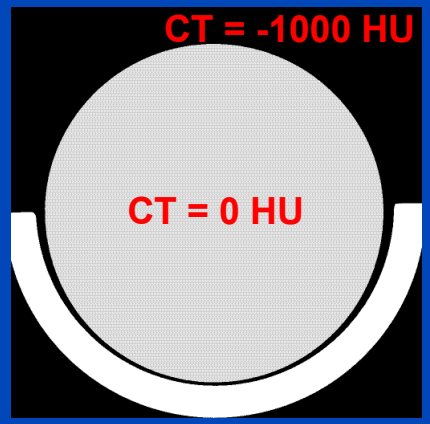

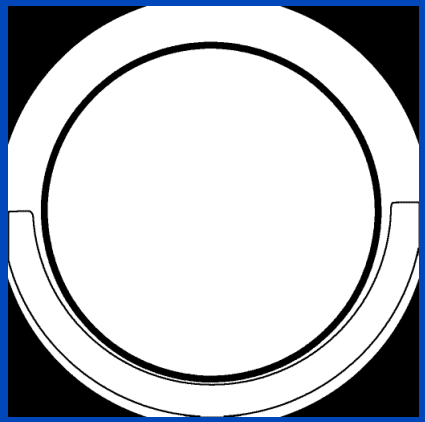

Original image $f_1(\boldsymbol{r})$

Template image $t(\boldsymbol{r})$

Weight image $w(\boldsymbol{r})$

M. Kachelrieß, K. Sourbelle, and W.A. Kalender, "Empirical cupping correction: A first-order raw data precorrection for cone-beam computed tomography," Med. Phys. 33(5):1269-1274, May 2006.

dkfz.

Results: Water Phantom

Orig (Mean±4Sigma)

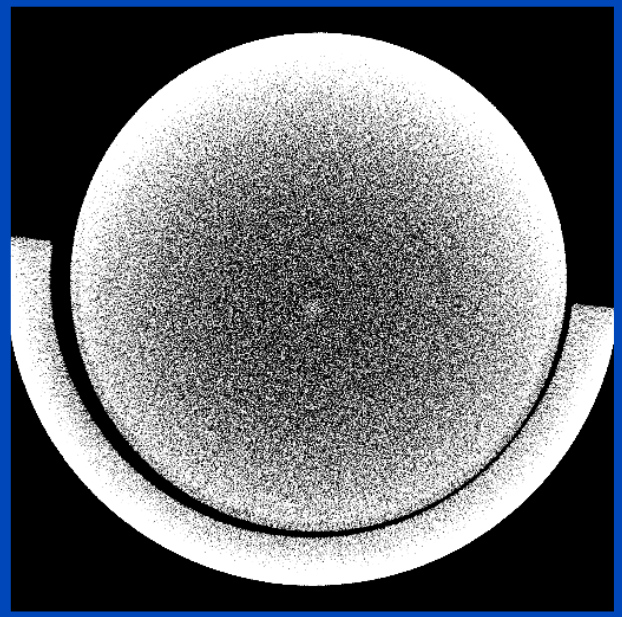

ECC (Mean±4Sigma)

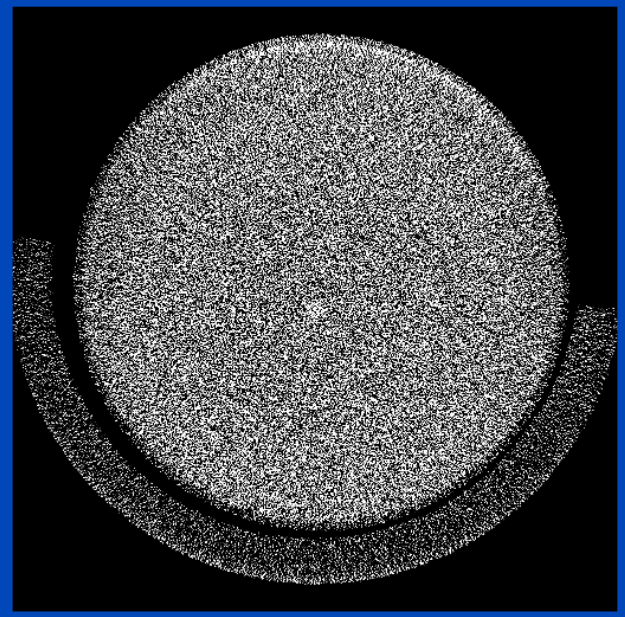

M. Kachelrieß, K. Sourbelle, and W.A. Kalender, “Empirical cupping correction: A first-order raw data precorrection for cone-beam computed tomography,” Med. Phys. 33(5):1269-1274, May 2006.

Results: Mouse Scan

No correction (Mean±4Sigma)

ECC (Mean±4Sigma)

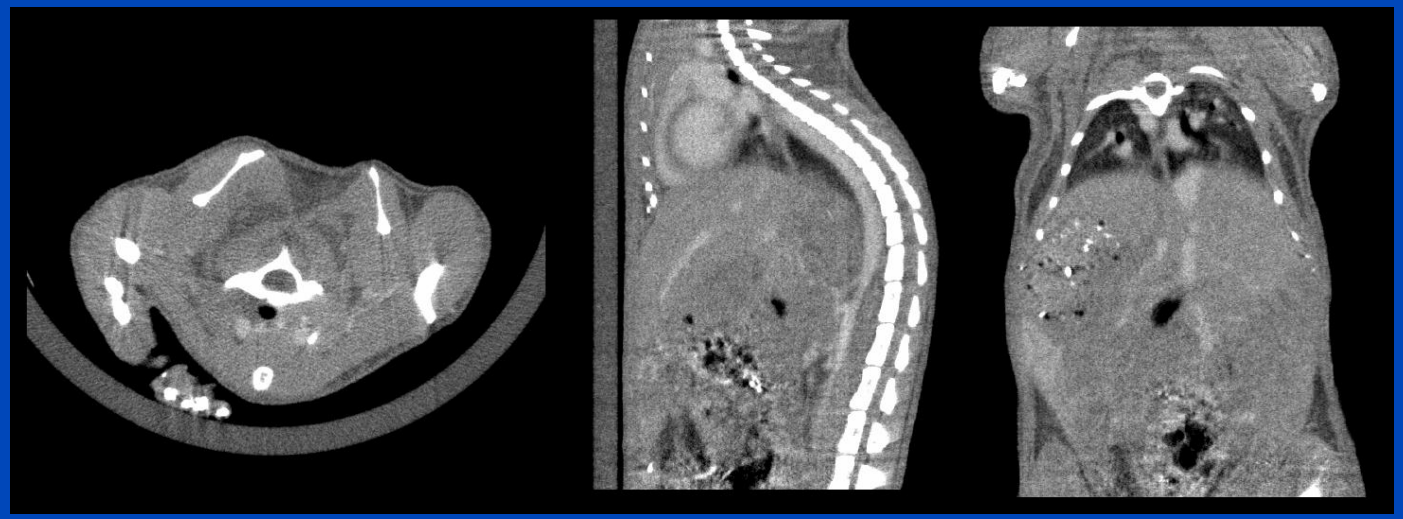

M. Kachelrieß, K. Sourbelle, and W.A. Kalender, “Empirical cupping correction: A first-order raw data precorrection for cone-beam computed tomography,” Med. Phys. 33(5):1269-1274, May 2006.

dkfz.

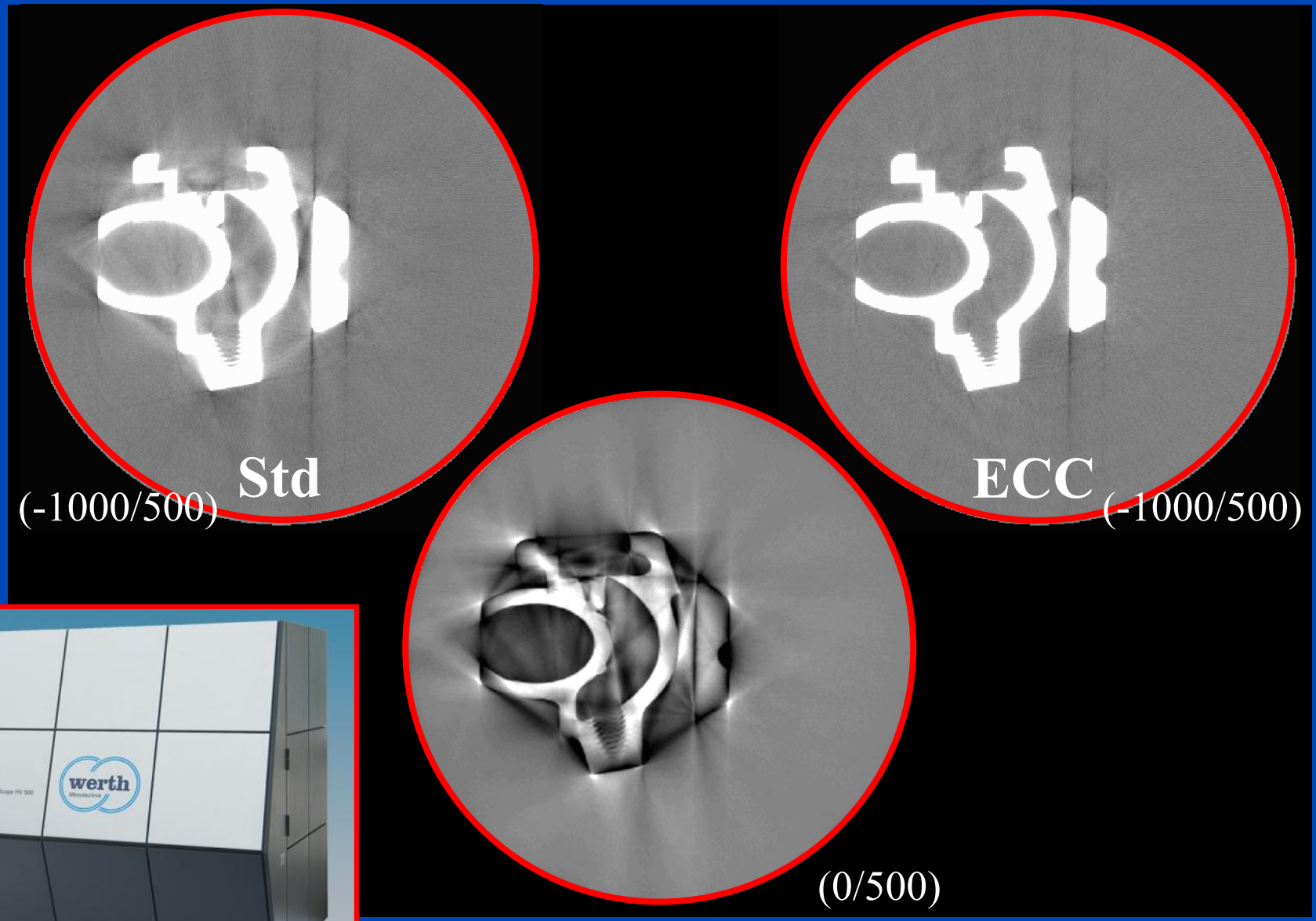

CT Metrology

M. Kachelrieß, K. Sourbelle, and W.A. Kalender, "Empirical cupping correction: A first-order raw data precorrection for cone-beam computed tomography," Med. Phys. 33(5):1269-1274, May 2006.

dkfz.

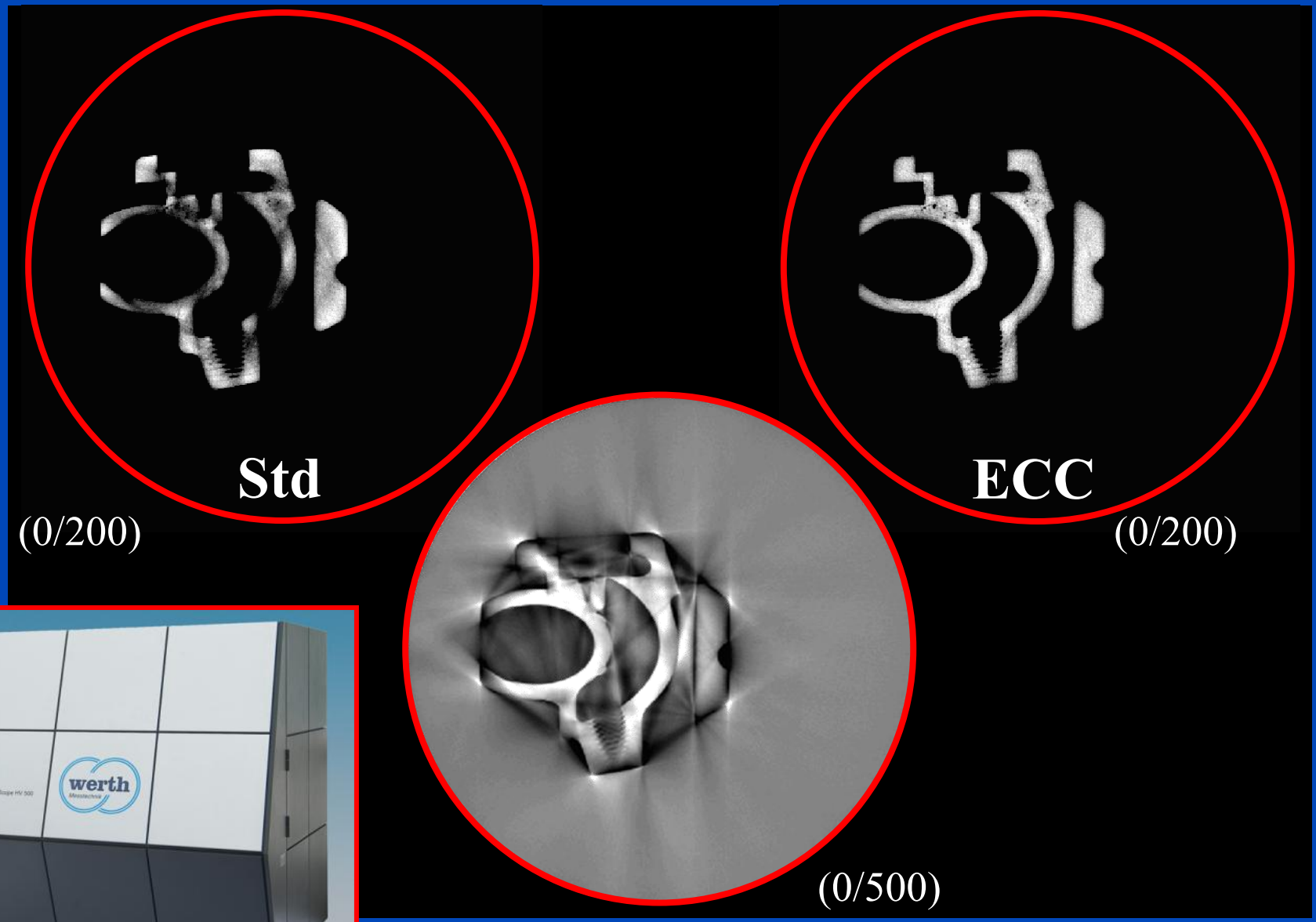

CT Metrology

M. Kachelrieß, K. Sourbelle, and W.A. Kalender, "Empirical cupping correction: A first-order raw data precorrection for cone-beam computed tomography," Med. Phys. 33(5):1269-1274, May 2006.

dkfz.

Empirical binary tomography calibration (EBTC) for the precorrection of beam hardening and scatter for flat panel CT

Rainer Grimmer[a)] and Marc Kachelrieß
Institute of Medical Physics, University of Erlangen-Nürnberg, Erlangen 91052, Germany

(Received 24 September 2010; revised 31 January 2011; accepted for publication 12 February 2011; published 30 March 2011)

Purpose: Scatter and beam hardening are prominent artifacts in x-ray CT. Currently, there is no precorrection method that inherently accounts for tube voltage modulation and shaped prefiltration.
Methods: A method for self-calibration based on binary tomography of homogeneous objects, which was proposed by B. Li *et al.* ["A novel beam hardening correction method for computed tomography," in Proceedings of the IEEE/ICME International Conference on Complex Medical Engineering CME 2007, pp. 891–895, 23–27 May 2007], has been generalized in order to use this information to preprocess scans of other, nonbinary objects, e.g., to reduce artifacts in medical CT applications. Further on, the method was extended to handle scatter besides beam hardening and to allow for detector pixel-specific and ray-specific precorrections. This implies that the empirical binary tomography calibration (EBTC) technique is sensitive to spectral effects as they are induced by the heel effect, by shaped prefiltration, or by scanners with tube voltage modulation. The presented method models the beam hardening correction by using a rational function, while the scatter component is modeled using the pep model of B. Ohnesorge *et al.* ["Efficient object scatter correction algorithm for third and fourth generation CT scanners," Eur. Radiol. **9**(3), 563–569 (1999)]. A smoothness constraint is applied to the parameter space to regularize the underdetermined system of nonlinear equations. The parameters determined are then used to precorrect CT scans.
Results: EBTC was evaluated using simulated data of a flat panel cone-beam CT scanner with tube voltage modulation and bow-tie prefiltration and using real data of a flat panel cone-beam CT scanner. In simulation studies, where the ground truth is known, the authors' correction model proved to be highly accurate and was able to reduce beam hardening by 97% and scatter by about 75%. Reconstructions of measured data showed significantly less artifacts than the standard reconstruction.
Conclusions: EBTC appears to be an efficient algorithm to precorrect CT raw data for beam hardening and scatter and it can account for ray-dependent spectral variations as they occur due to the heel effect, due to shaped prefiltration, or due to variations in tube voltage. [DOI: 10.1118/1.3561506]

R. Grimmer and M. Kachelrieß. Empirical binary tomography calibration (EBTC) for the precorrection of beam hardening and scatter for flat panel CT. Med. Phys. 38(4): 2234-2240, Feb. 2011.

dkfz.

Prior Art

- **Binary tomography for self calibration:**
  - B. Li, Q. Zhang, and J. Li, “A Novel Beam Hardening Correction Method for Computed Tomography," Proc. IEEE/ICME International Conference on Complex Medical Engineering CME 2007, pp. 891 – 895, 2007.
- **Beam hardening or scatter calibration:**
  - R. A. Brooks and G. D. Chiro, “Beam hardening in x-ray reconstructive," Phys. Med. Biol., vol. 21, pp. 390 – 398, 1976.
  - M. Kachelrieß, K. Sourbelle, and W. A. Kalender, “Empirical cupping correction: a first-order raw data precorrection for cone-beam computed tomography," Med. Phys., vol. 33, pp. 1269 – 1274, 2006.
  - J. Star-Lack, M. Sun, A. Kaestner, R. Hassanein, Gary Virshup, T. Berkus, and M. Oelhafen, “Efficient scatter correction using asymmetric kernels," Proc. of SPIE Vol. 7258, pp. 72581Z, 2009.

EBTC: Basic Idea

- Compare measurement of a binary object with forward projection of its segmented binary image.
- Fit nonlinear models for every detector element: E.g.
  - a rational function to model polychromacy
  - the pep-model[1] to model scatter
- Use the calibrated parameters to preprocess other data.

[1]Ohnesorge et al., Eur. Radiol., pp. 563 – 569, 1999

EBTC Properties

- Calibration measurement of a phantom of one material with constant density
- Phantom geometry can be unknown
- Tube voltage modulation is allowed
- Bow tie filtration and heel effect are compensated for

R. Grimmer and M. Kachelrieß. Empirical binary tomography calibration (EBTC)
for the precorrection of beam hardening and scatter for flat panel CT. Med. Phys. 38(4): 2234-2240, Feb. 2011.

Beam Hardening Model

- To correct for the beam hardening effects a rational function was used due to its good asymptotic behavior
- The function

$$p = \frac{c_0 + c_1 q + c_2 q^2 + c_3 q^3}{1 + c_4 q + c_5 q^2}$$

  maps the measured polychromatic attenuation values *q* to the ideal monochromatic values *p*.
- EBTC estimates c_0, c_1, …, c_5.

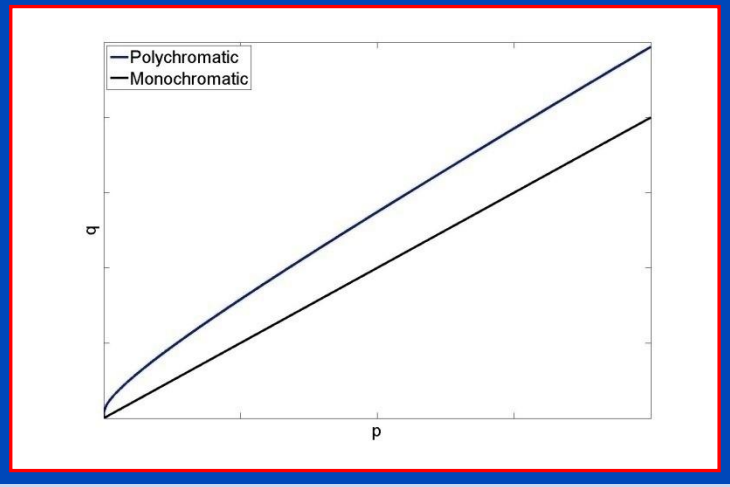

R. Grimmer and M. Kachelrieß. Empirical binary tomography calibration (EBTC) for the precorrection of beam hardening and scatter for flat panel CT. Med. Phys. 38(4): 2234-2240, Feb. 2011.

dkfz.

Scatter Correction Model

- To correct for scatter, the beam hardening corrected data are passed through

$$p = -\ln\left(e^{-q} - qe^{-q} * \left(s_0 + s_1 e^{-s_2 u^2 - s_3 v^2}\right)\right)$$

where s_0, s_1, s_2, and s_3, are estimated by EBTC.

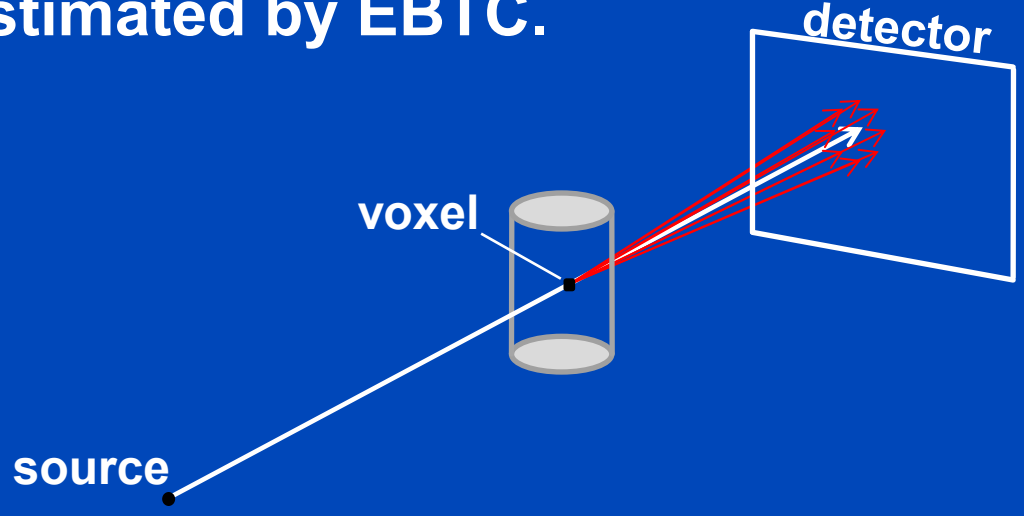

R. Grimmer and M. Kachelrieß. Empirical binary tomography calibration (EBTC) for the precorrection of beam hardening and scatter for flat panel CT. Med. Phys. 38(4): 2234-2240, Feb. 2011.

Basic Concept

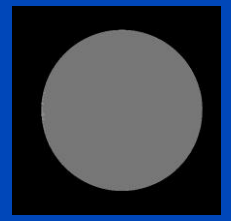
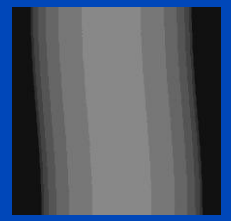
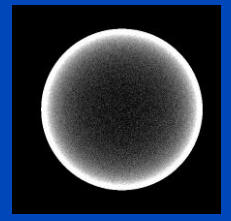
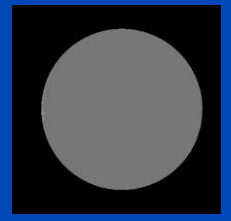
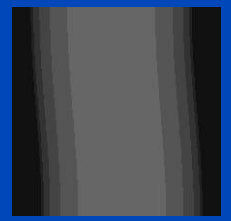

Calibration Object

Acquisition

Sinogram

Reconstruction

Reconstructed Image

Segmentation

Binary Image

Forward Projection

Artificial Sinogram

LM Parameter Estimation

10 parameters per reading with smoothness constraint

Measured Sinogram

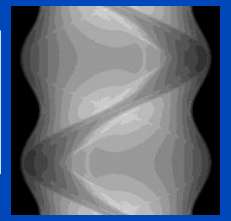

Reconstruction

Normal Image

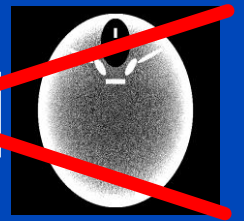

Correction Coeffs

Modification

Corrected Sinogram

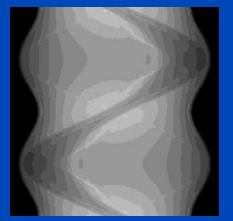

Reconstruction

Corrected Image

R. Grimmer and M. Kachelrieß. Empirical binary tomography calibration (EBTC) for the precorrection of beam hardening and scatter for flat panel CT. Med. Phys. 38(4): 2234-2240, Feb. 2011.

dkfz.

Simulation Setup

- Tube voltage modulation is artificially applied with sinusoidal shape from 100 kV down to 60 kV over 90°

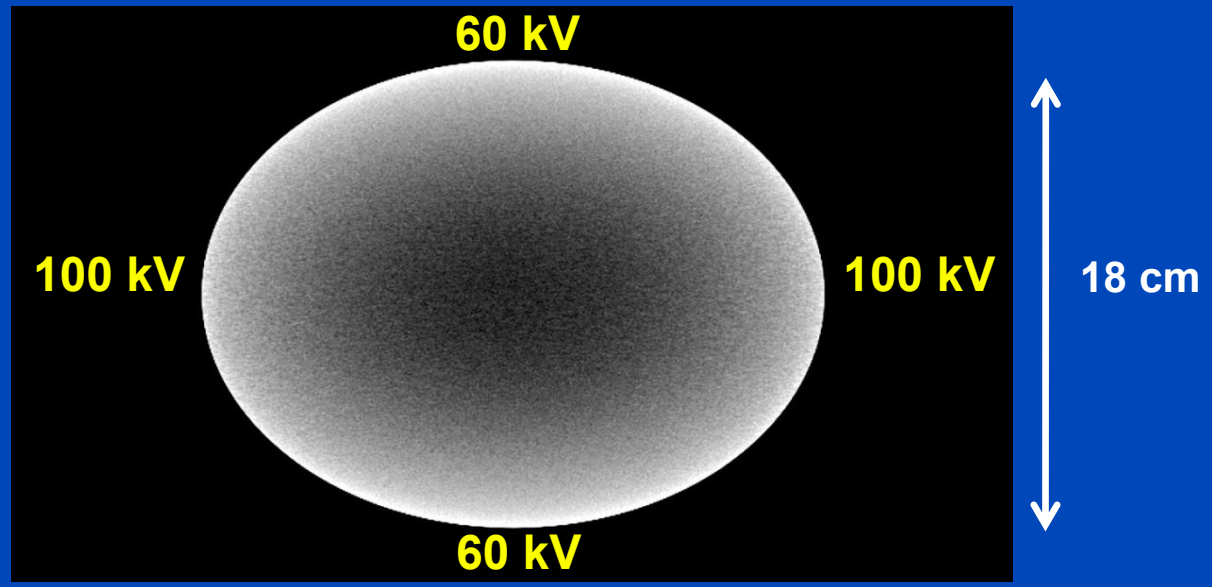

- Scatter is modeled by using a Monte-Carlo simulation with multiple photon interactions.

R. Grimmer and M. Kachelrieß. Empirical binary tomography calibration (EBTC) for the precorrection of beam hardening and scatter for flat panel CT. Med. Phys. 38(4): 2234-2240, Feb. 2011.

Simulation Results – Head Phantom

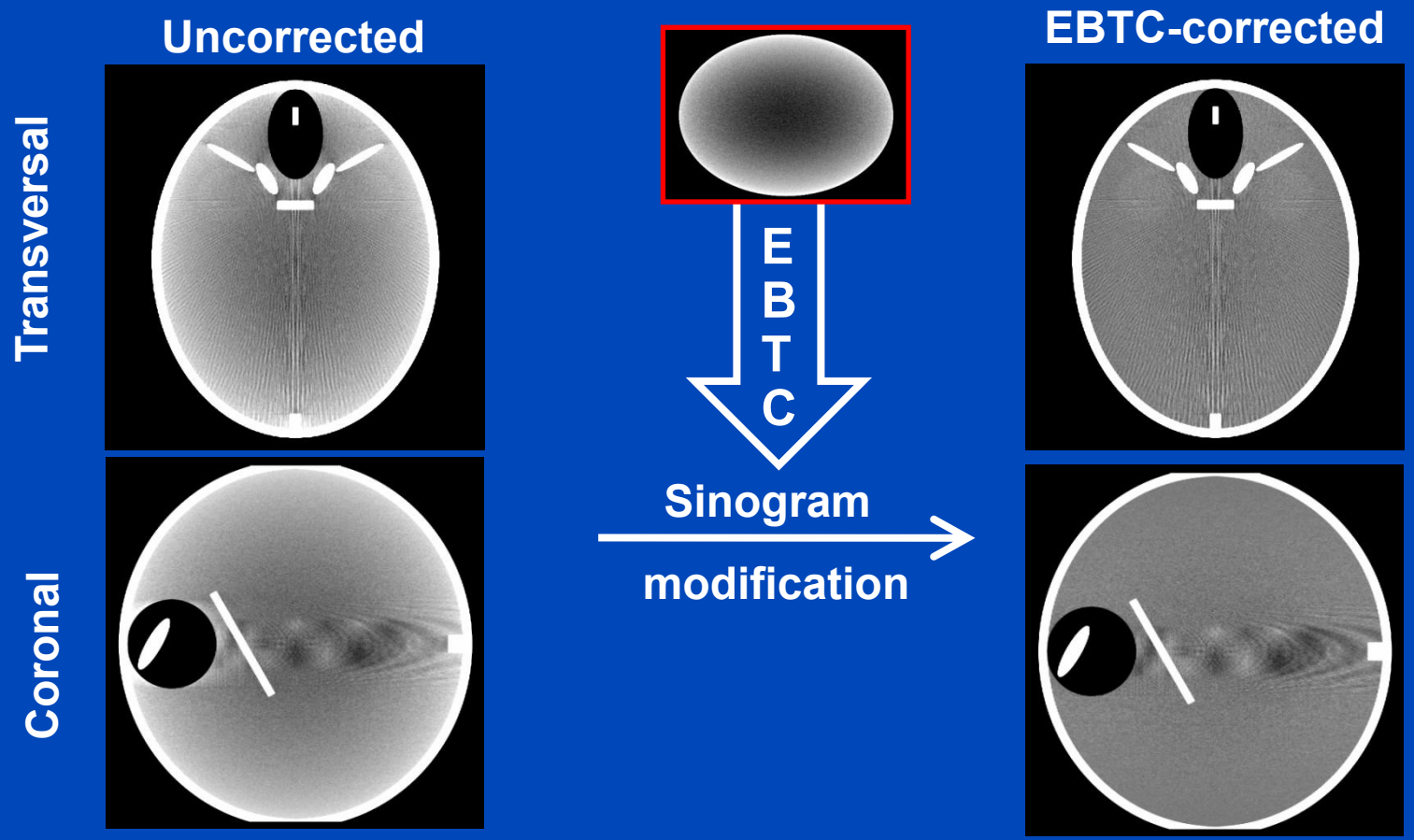

W = 400 HU

R. Grimmer and M. Kachelrieß. Empirical binary tomography calibration (EBTC) for the precorrection of beam hardening and scatter for flat panel CT. Med. Phys. 38(4): 2234-2240, Feb. 2011.

dkfz.

Simulation Results – Thorax Phantom

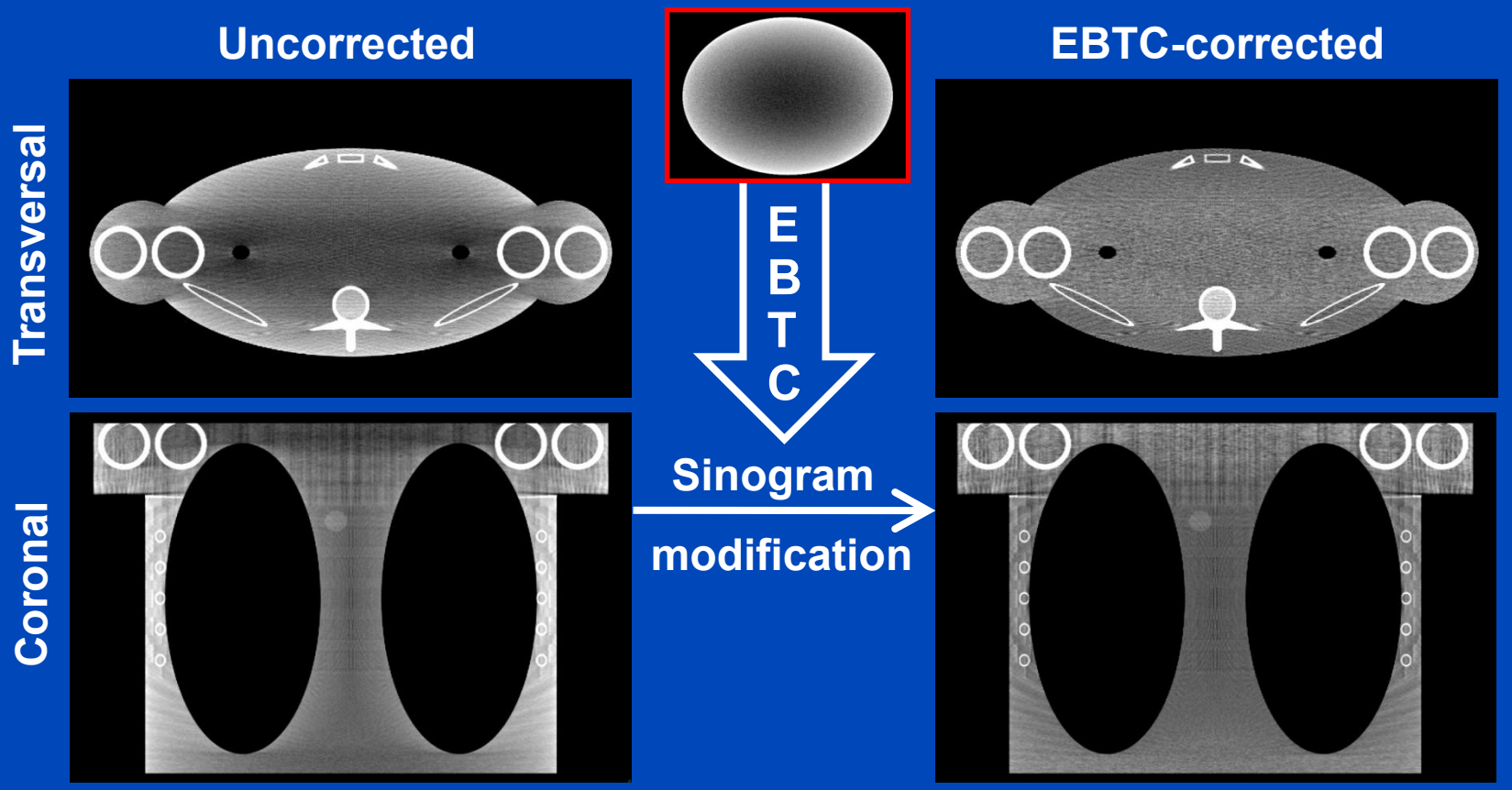

W = 500 HU

R. Grimmer and M. Kachelrieß. Empirical binary tomography calibration (EBTC) for the precorrection of beam hardening and scatter for flat panel CT. Med. Phys. 38(4): 2234-2240, Feb. 2011.

dkfz.

Measured Data – Water Phantom

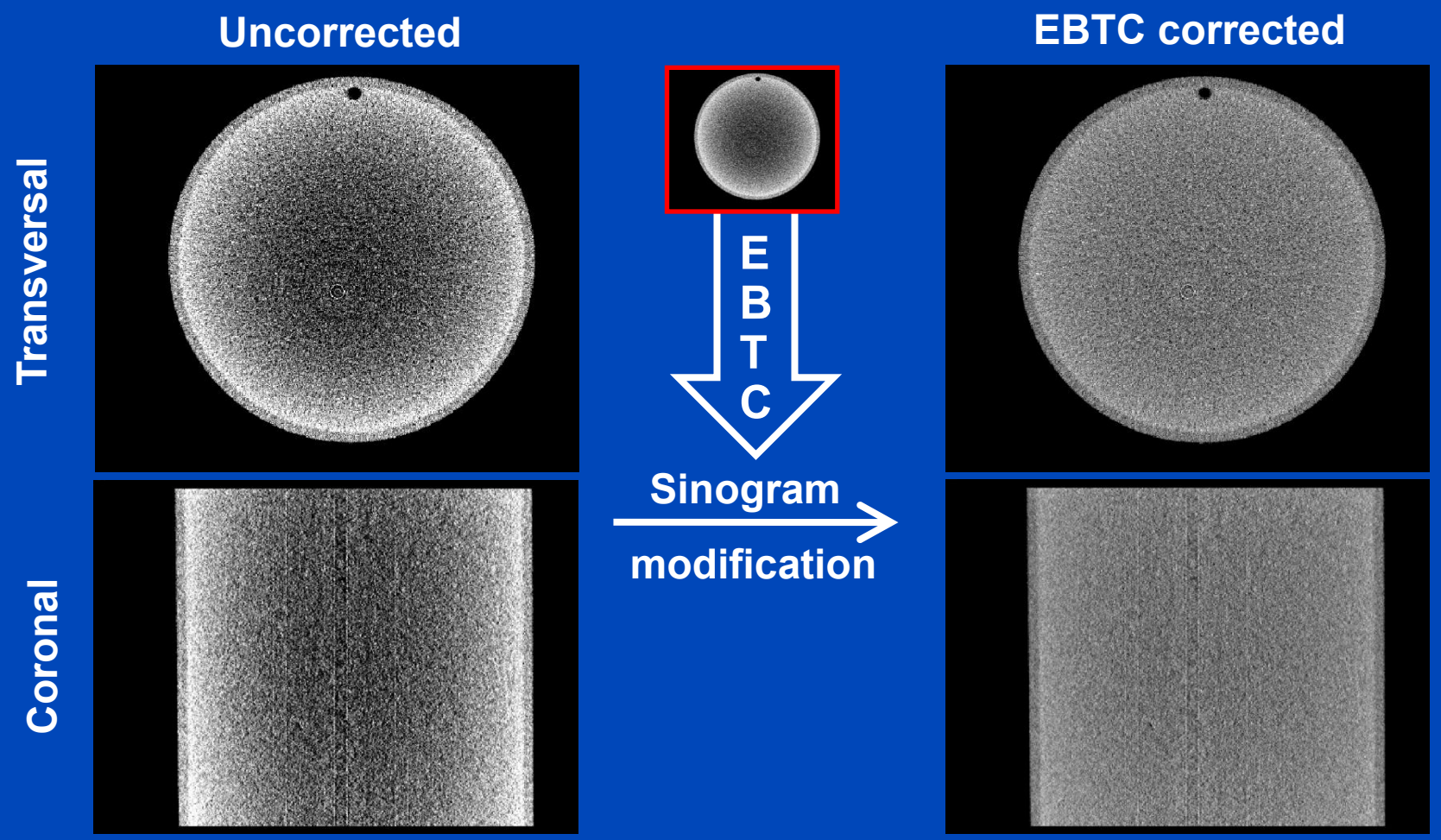

TomoScope micro-CT, 40 kV, 32 mm water cylinder, W = 500 HU

R. Grimmer and M. Kachelrieß. Empirical binary tomography calibration (EBTC) for the precorrection of beam hardening and scatter for flat panel CT. Med. Phys. 38(4): 2234-2240, Feb. 2011.

dkfz.

Measured Data – Mouse

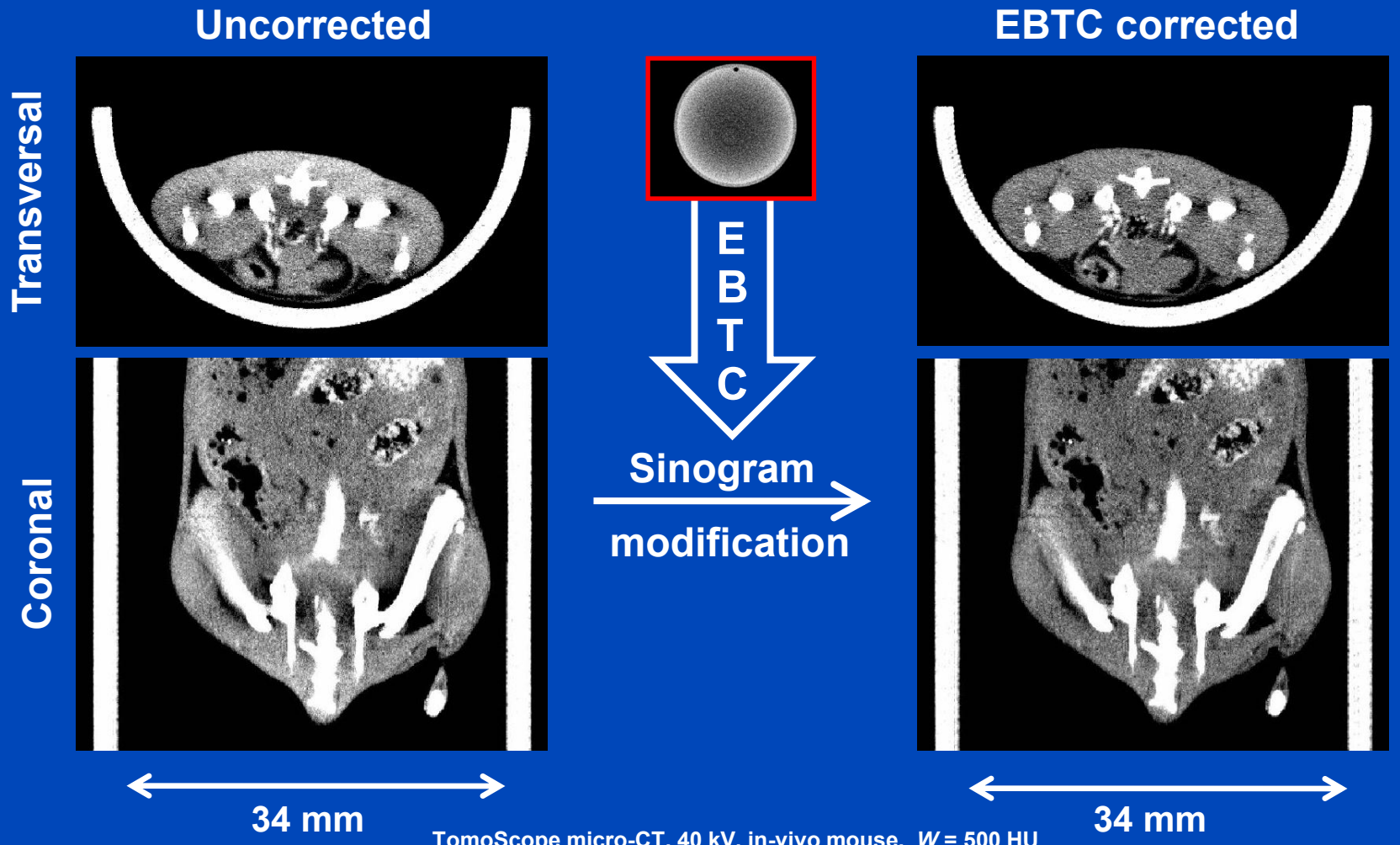

TomoScope micro-CT, 40 kV, in-vivo mouse, W = 500 HU

R. Grimmer and M. Kachelrieß. Empirical binary tomography calibration (EBTC) for the precorrection of beam hardening and scatter for flat panel CT. Med. Phys. 38(4): 2234-2240, Feb. 2011.

HIGHER ORDER BEAM HARDENING CORRECTION

CT-Values at Different Energies

	70 keV	100 keV	130 keV	160 keV
Water	0 HU	0 HU	0 HU	0 HU
Aluminum (Z=13)	2,000 HU	1,700 HU	1,500 HU	1,400 HU
Iron (Z=26)	32,000 HU	16,000 HU	11,000 HU	9,000 HU
Iodine (Z=53)	128,000 HU	55,000 HU	30,000 HU	19,000 HU

Values are rounded, for convenience.

Higher Order Beam Hardening

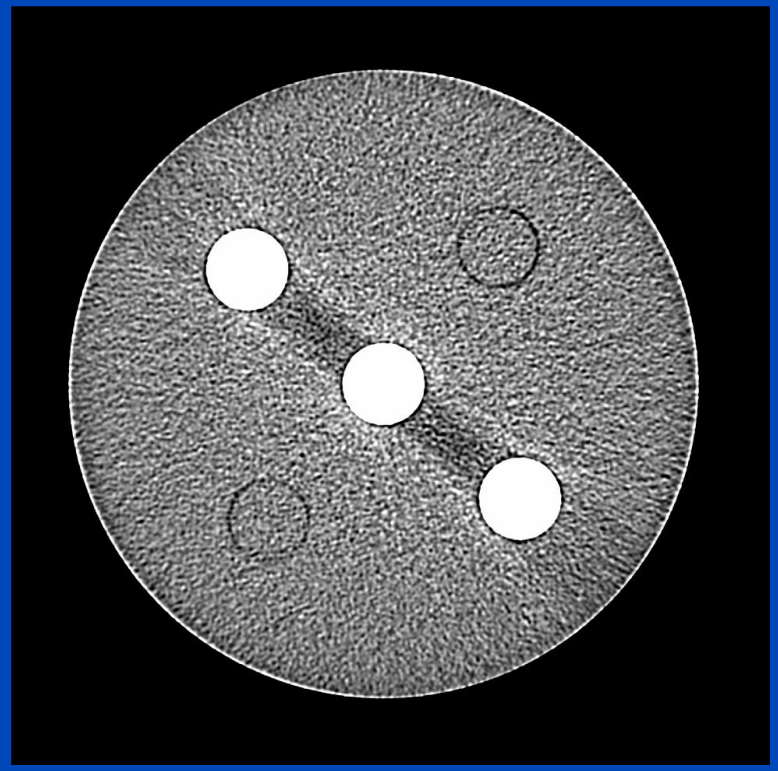

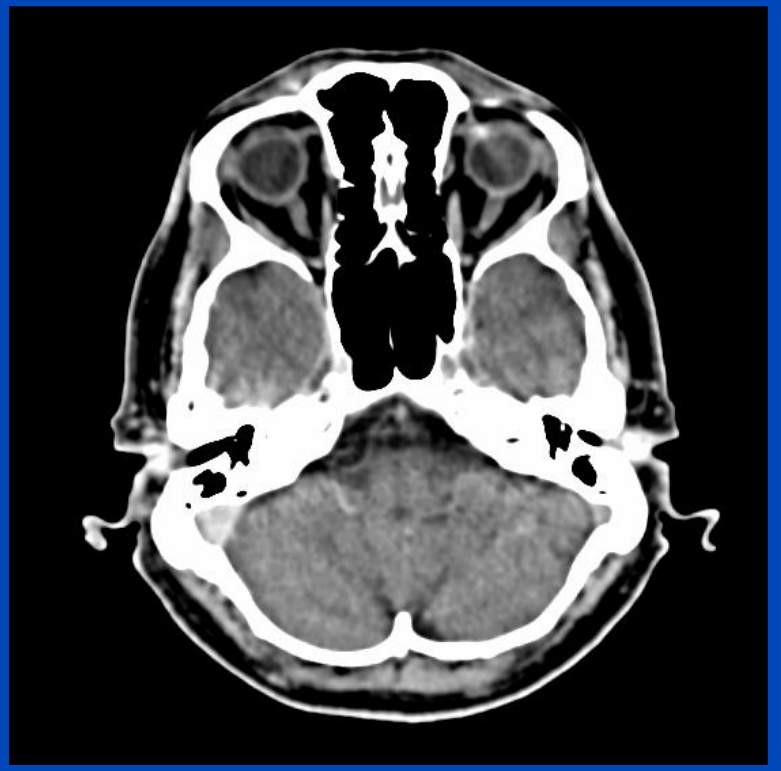

Image domain algorithms, such as the scaling method, do not account for higher order beam hardening effects. They can recover the attenuation correction factors (ACF) only to a first order of approximation.

M. Kachelrieß, and W.A. Kalender, "Improving PET/CT attenuation correction with iterative CT beam hardening correction," IEEE Medical Imaging Conference Program, M04-5, October 2005.

Energy Dependence of Attenuation

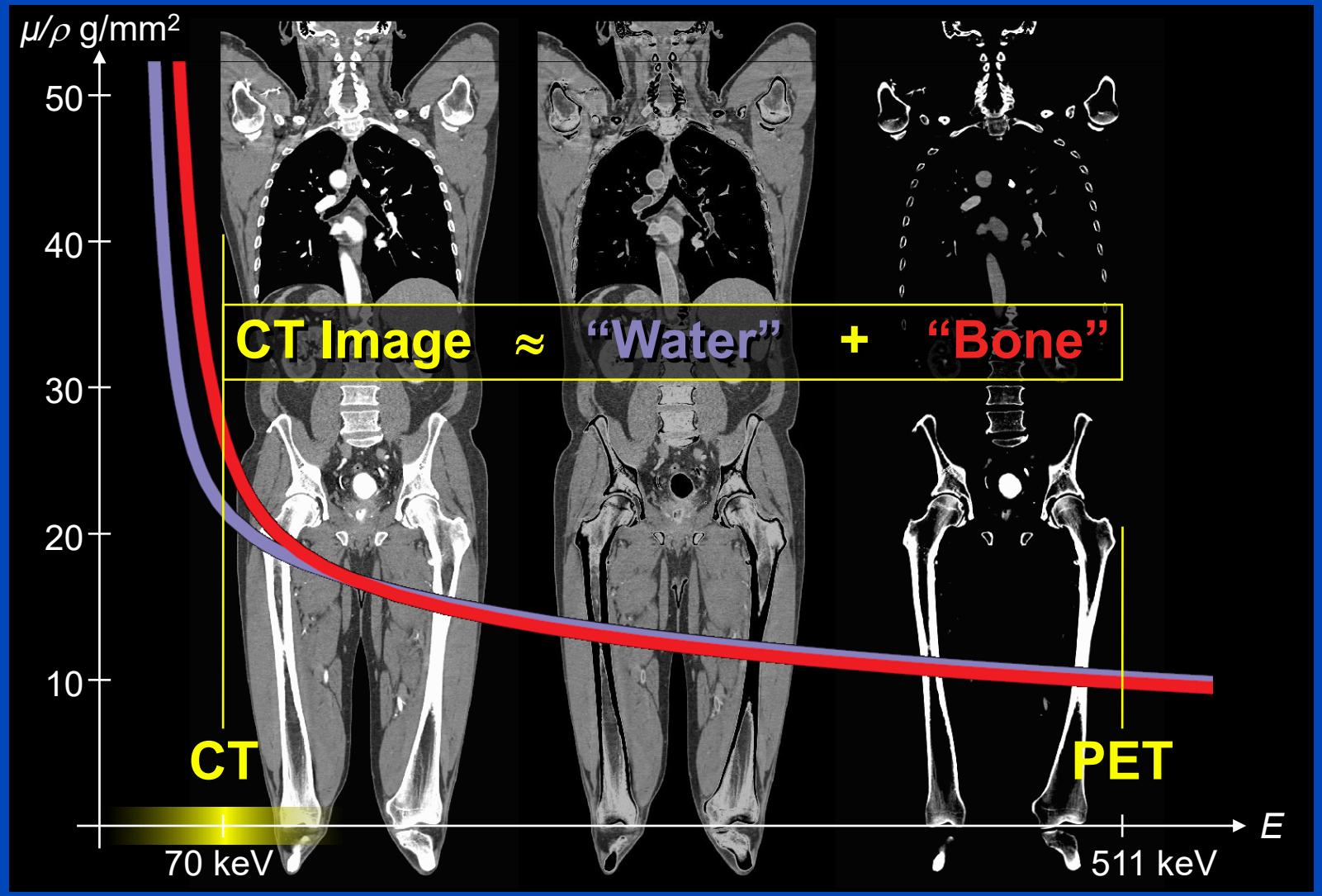

M. Kachelrieß, and W.A. Kalender, "Improving PET/CT attenuation correction with iterative CT beam hardening correction," IEEE Medical Imaging Conference Program, M04-5, October 2005.

dkfz.

Many Materials
(typically requires iterative BHC)

- **Assume** $\mu(E, \boldsymbol{r}) = \sum_i \psi_i(E) g_i(\boldsymbol{r}) = \boldsymbol{\psi}(E) \cdot \boldsymbol{g}(\boldsymbol{r})$
- **Let** $q = \mathsf{X}_g g = -\ln \int dE\, w(E) e^{-\boldsymbol{\psi}(E) \cdot \boldsymbol{p}}$

  with $p_i = \mathsf{X} g_i = \int dL\, g_i(\boldsymbol{r})$

- **For beam hardening correction we need to recover $g_i(r)$ for all materials present. Then we can convert to any desired E_0 as**

$$\mu(E_0, \boldsymbol{r}) = \sum_i \psi_i(E_0) g_i(\boldsymbol{r})$$

M. Kachelrieß, and W.A. Kalender, "Improving PET/CT attenuation correction with iterative CT beam hardening correction," IEEE Medical Imaging Conference Program, M04-5, October 2005.

Iterative BHC

initial water-precorrected CT image (or rawdata)

desired BHC-corrected CT image

$$\mathsf{X}_f f = \mathsf{X}_g g$$

$$\mathsf{B}_f f = \mathsf{B}_g g = g - (1 - \mathsf{B}_g) g$$

$$g = \mathsf{B}_f f + (1 - \mathsf{B}_g) g$$

with

$$\mathsf{B}_f = \mathsf{X}^{-1}\mathsf{X}_f$$

$$\mathsf{B}_g = \mathsf{X}^{-1}\mathsf{X}_g$$

Numerically superior expressions:

$$g = f + (\mathsf{B}_f - \mathsf{B}) f + (\mathsf{B} - \mathsf{B}_g) g \quad \text{with} \quad \mathsf{B} = \mathsf{X}^{-1}\mathsf{X}$$

$$g^{(n+1)} = f + (\mathsf{B}_f - \mathsf{B}) f + (\mathsf{B} - \mathsf{B}_g) g^{(n)} \quad \text{with} \quad g^{(0)} = f$$

Shortcut: $$g^{(1)} = f + \mathsf{X}^{-1}(\mathsf{X}_f - \mathsf{X}_g) f$$

M. Kachelrieß, and W.A. Kalender, “Improving PET/CT attenuation correction with iterative CT beam hardening correction,” IEEE Medical Imaging Conference Program, M04-5, October 2005.

Phantom Measurements

Spiral 64-Slice CT Scan at 120 kV

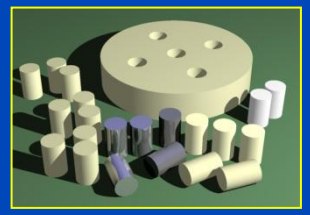

Original Image	BHC Image	Original minus BHC
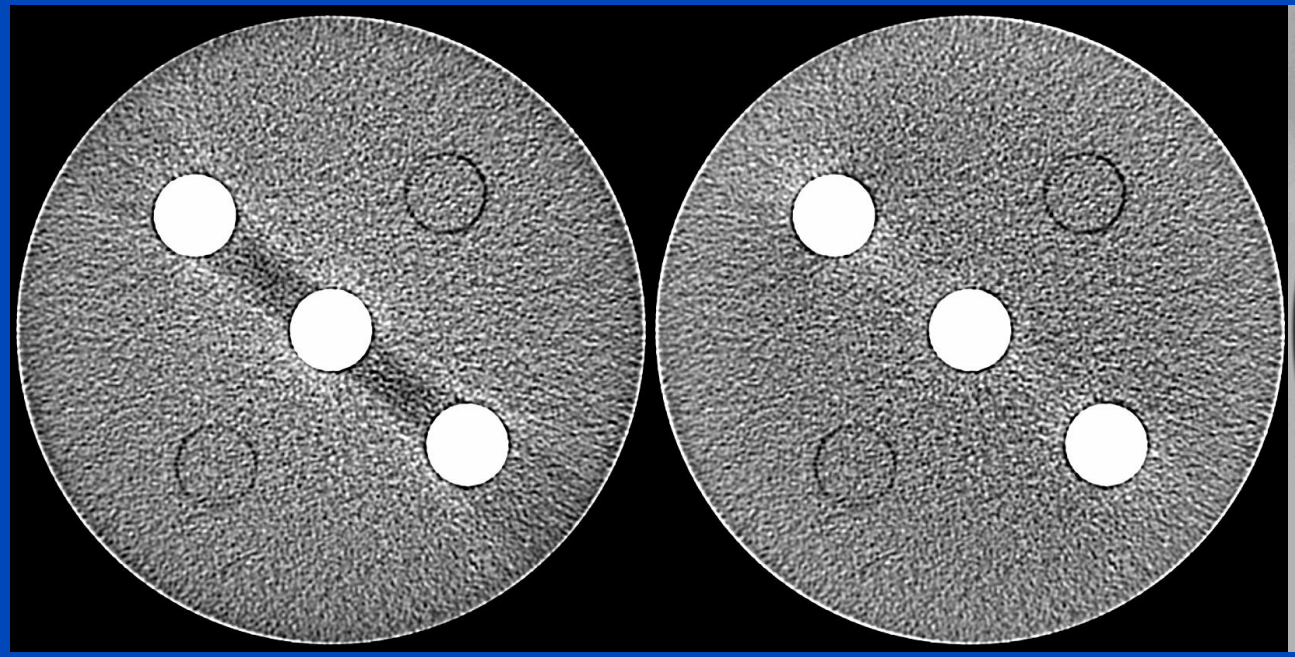		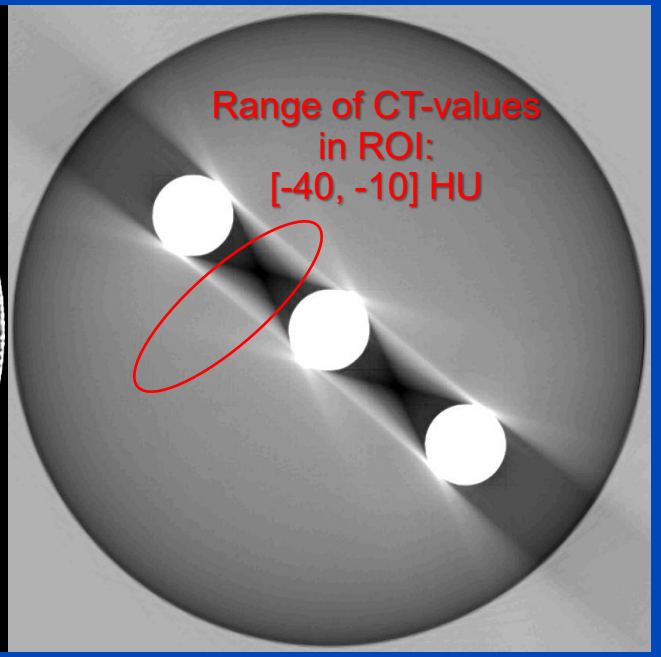
(*C* = -80 HU , *W* = 100 HU)	(*C* = -70 HU, *W* = 100 HU)	(*C* = -10 HU, *W* = 50 HU)

- 20 cm PE disk phantom with three 3 cm HA400 inserts
- BH artifacts apparent even for this small phantom
- BHC removes capping
- BHC removes dark streaks
- BHC recovers the true CT values

$$\rho_{\mathrm{PE}} = 0.93\,\rho_{\mathrm{W}} = -70\ \mathrm{HU}$$

$$\rho_{\mathrm{HA400}} = 1.27\rho_{\mathrm{W}} = 270\ \mathrm{HU}$$

Patient Data

Spiral 4-Slice CT Scan at 120 kV

Original Image

BHC Image

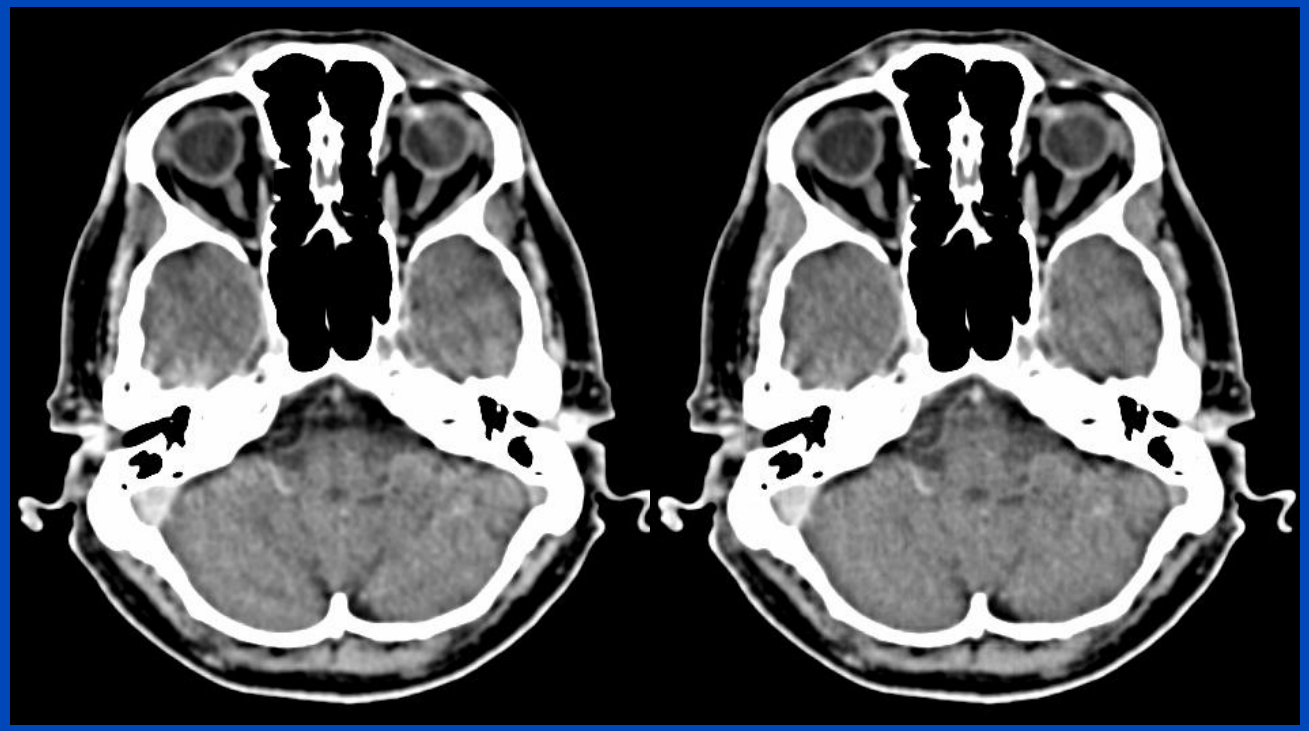

(*C* = 40 HU, *W* = 150 HU)

Original minus BHC

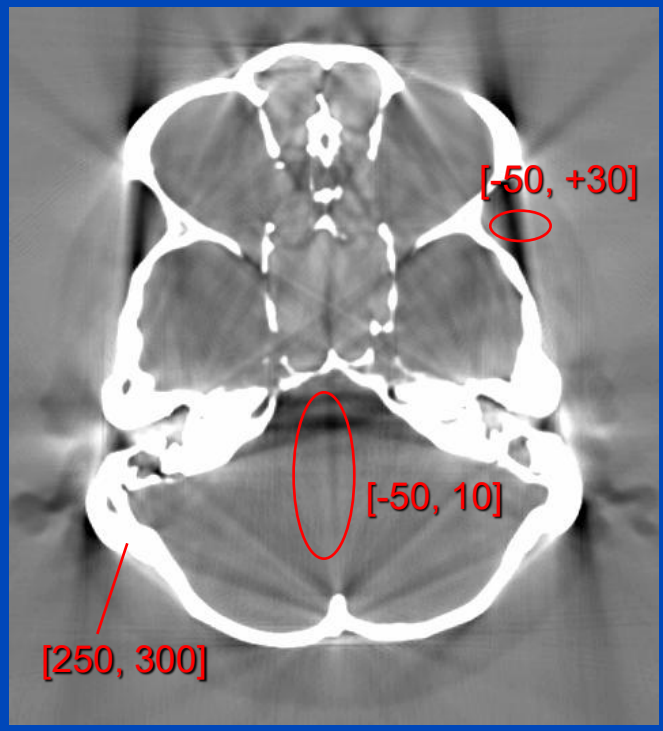

(*C* = 0 HU, *W* = 100 HU)

Red values indicate the range of CT-values within the corresponding ROI in HU

M. Kachelrieß, and W.A. Kalender, "Improving PET/CT attenuation correction with iterative CT beam hardening correction," IEEE Medical Imaging Conference Program, M04-5, October 2005.

dkfz.

Empirical beam hardening correction (EBHC) for CT

Yiannis Kyriakou, Esther Meyer, Daniel Prell, and Marc Kachelrieß[a)]
Institute of Medical Physics, University of Erlangen–Nürnberg, 91052 Erlangen, Germany

(Received 19 May 2010; revised 1 July 2010; accepted for publication 13 July 2010; published 8 September 2010)

Purpose: Due to x-ray beam polychromaticity and scattered radiation, attenuation measurements tend to be underestimated. Cupping and beam hardening artifacts become apparent in the reconstructed CT images. If only one material such as water, for example, is present, these artifacts can be reduced by precorrecting the rawdata. Higher order beam hardening artifacts, as they result when a mixture of materials such as water and bone, or water and bone and iodine is present, require an iterative beam hardening correction where the image is segmented into different materials and those are forward projected to obtain new rawdata. Typically, the forward projection must correctly model the beam polychromaticity and account for all physical effects, including the energy dependence of the assumed materials in the patient, the detector response, and others. We propose a new algorithm that does not require any knowledge about spectra or attenuation coefficients and that does not need to be calibrated. The proposed method corrects beam hardening in single energy CT data.

Methods: The only *a priori* knowledge entering EBHC is the segmentation of the object into different materials. Materials other than water are segmented from the original image, e.g., by using simple thresholding. Then, a (monochromatic) forward projection of these other materials is performed. The measured rawdata and the forward projected material-specific rawdata are monomially combined (e.g., multiplied or squared) and reconstructed to yield a set of correction volumes. These are then linearly combined and added to the original volume. The combination weights are determined to maximize the flatness of the new and corrected volume. EBHC is evaluated using data acquired with a modern cone-beam dual-source spiral CT scanner (Somatom Definition Flash, Siemens Healthcare, Forchheim, Germany), with a modern dual-source micro-CT scanner (TomoScope Synergy Twin, CT Imaging GmbH, Erlangen, Germany), and with a modern C-arm CT scanner (Axiom Artis dTA, Siemens Healthcare, Forchheim, Germany). A large variety of phantom, small animal, and patient data were used to demonstrate the data and system independence of EBHC.

Results: Although no physics apart from the initial segmentation procedure enter the correction process, beam hardening artifacts were significantly reduced by EBHC. The image quality for clinical CT, micro-CT, and C-arm CT was highly improved. Only in the case of C-arm CT, where high scatter levels and calibration errors occur, the relative improvement was smaller.

Conclusions: The empirical beam hardening correction is an interesting alternative to conventional iterative higher order beam hardening correction algorithms. It does not tend to over- or undercorrect the data. Apart from the segmentation step, EBHC does not require assumptions on the spectra or on the type of material involved. Potentially, it can therefore be applied to any CT image. [DOI: 10.1118/1.3477088]

Key words: Computed tomography (CT), beam hardening correction, x-ray, scatter

Empirical Beam Hardening Correction (EBHC)

- **Requirements/Objectives**
  - Empirical correction of higher order beam hardening effects
  - No assumptions on attenuation coefficients, spectra, detector responses or other properties of the scanner
  - Image-based and system-independent method

- **Overview of correction steps**
  - Forward project segmented bone volume to obtain artificial rawdata
  - Pass the artificial rawdata through basis functions
  - Reconstruct the basis functions
  - Linearly combine the correction volumes and the original volume using flatness maximization

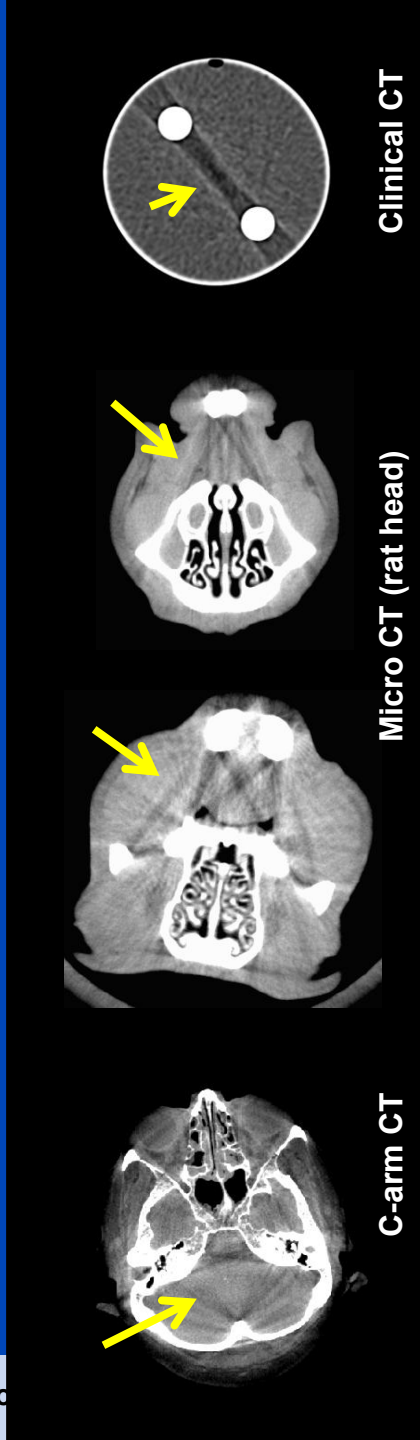

Y. Kyriakou, E. Meyer, D. Prell, and M. Kachelrieß, "Empirical beam hardening correction (EBHC) for CT," Med. Phys. 37(10):5179-5187, Octo

EBHC Details

- **Decomposition into an effective water-equivalent density $\hat{f}_1(r)$ of the object and into an effective energy dependence $\hat{\psi}_2(E)$ of a second material, e.g. bone**

$$\begin{aligned}\mu(\boldsymbol{r}, E) &= f_1(\boldsymbol{r})\psi_1(E) + f_2(\boldsymbol{r})\psi_2(E) \\ &= \big(f_1(\boldsymbol{r}) + f_2(\boldsymbol{r})\big)\psi_1(E) + f_2(\boldsymbol{r})\big(\psi_2(E) - \psi_1(E)\big) \\ &= \hat{f}_1(\boldsymbol{r})\psi_1(E) + f_2(\boldsymbol{r})\hat{\psi}_2(E).\end{aligned}$$

- **Assuming water-precorrected data gives**

$$\int dE\, w(E) e^{-p_0\psi_0(E)} = \int dE\, w(E) e^{-\hat{p}_1\psi_1(E) - p_2\hat{\psi}_2(E)}.$$

where $\hat{p}_1$ and p_2 are the line integrals through $\hat{f}_1(r)$ and $f_2(\boldsymbol{r})$, respectively.

Y. Kyriakou, E. Meyer, D. Prell, and M. Kachelrieß, "Empirical beam hardening correction (EBHC) for CT," Med. Phys. 37(10):5179-5187, October 2010.

EBHC Details

- **Assuming $\psi_1(E) = \psi_0(E)$ solve for $\hat{p}_1$ using a series expansion**

$$\hat{p}_1(p_0, p_2) = p_0 + c_{01}p_2 + c_{11}p_0p_2 + c_{02}p_2^2 + \dots$$

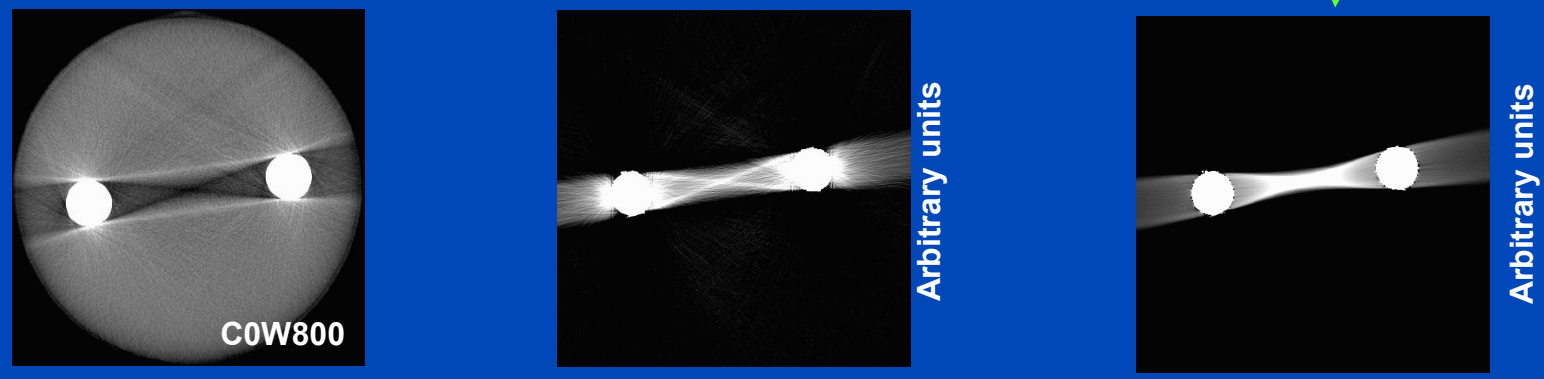

- **Empirically find c_{11} and c_{02} to correct initial image by flatness maximization**

Y. Kyriakou, E. Meyer, D. Prell, and M. Kachelrieß, "Empirical beam hardening correction (EBHC) for CT," Med. Phys. 37(10):5179-5187, October 2010.

EBHC for Clinical CT

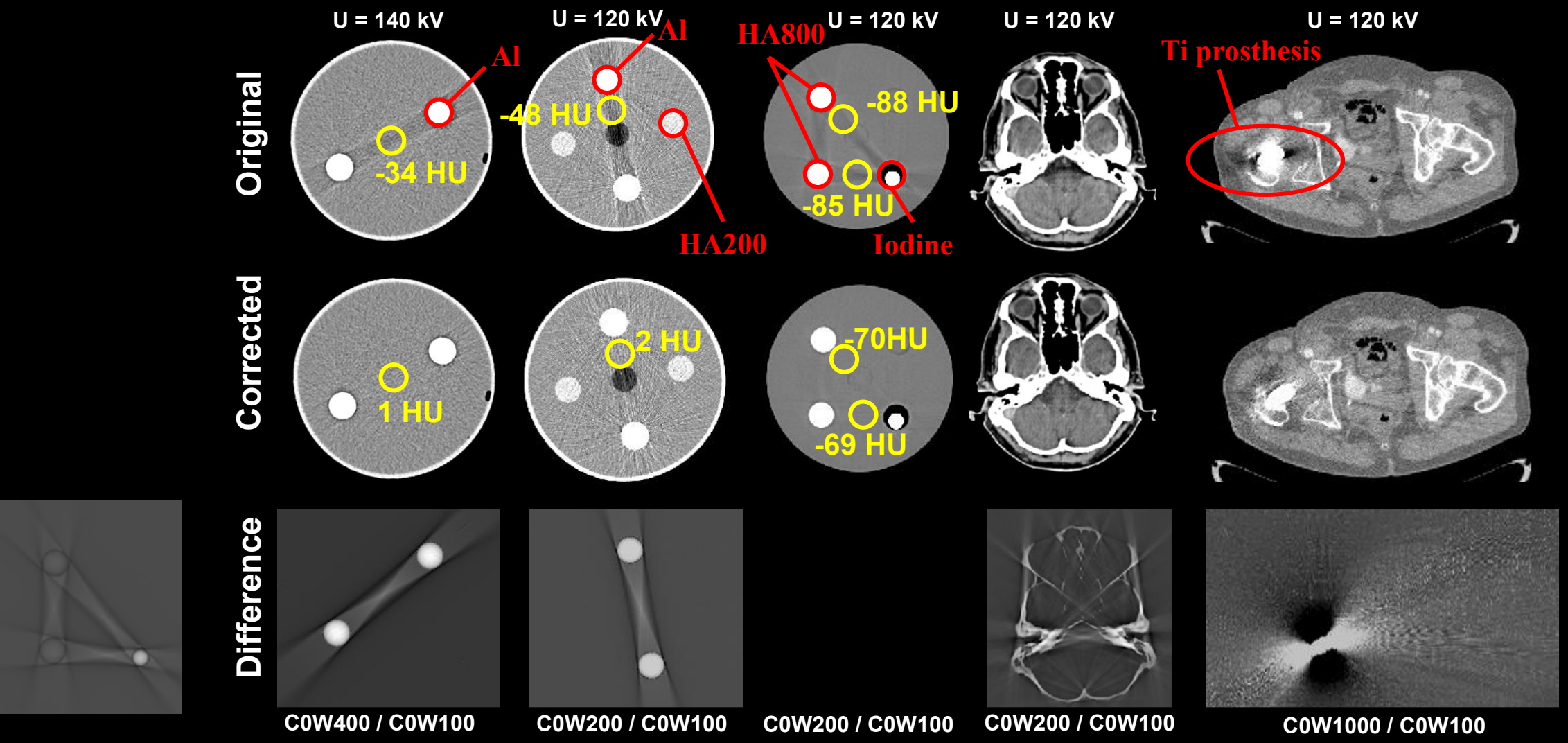

Y. Kyriakou, E. Meyer, D. Prell, and M. Kachelrieß, "Empirical beam hardening correction (EBHC) for CT," Med. Phys. 37(10):5179-5187, October 2010.

dkfz.

EBHC for Micro CT

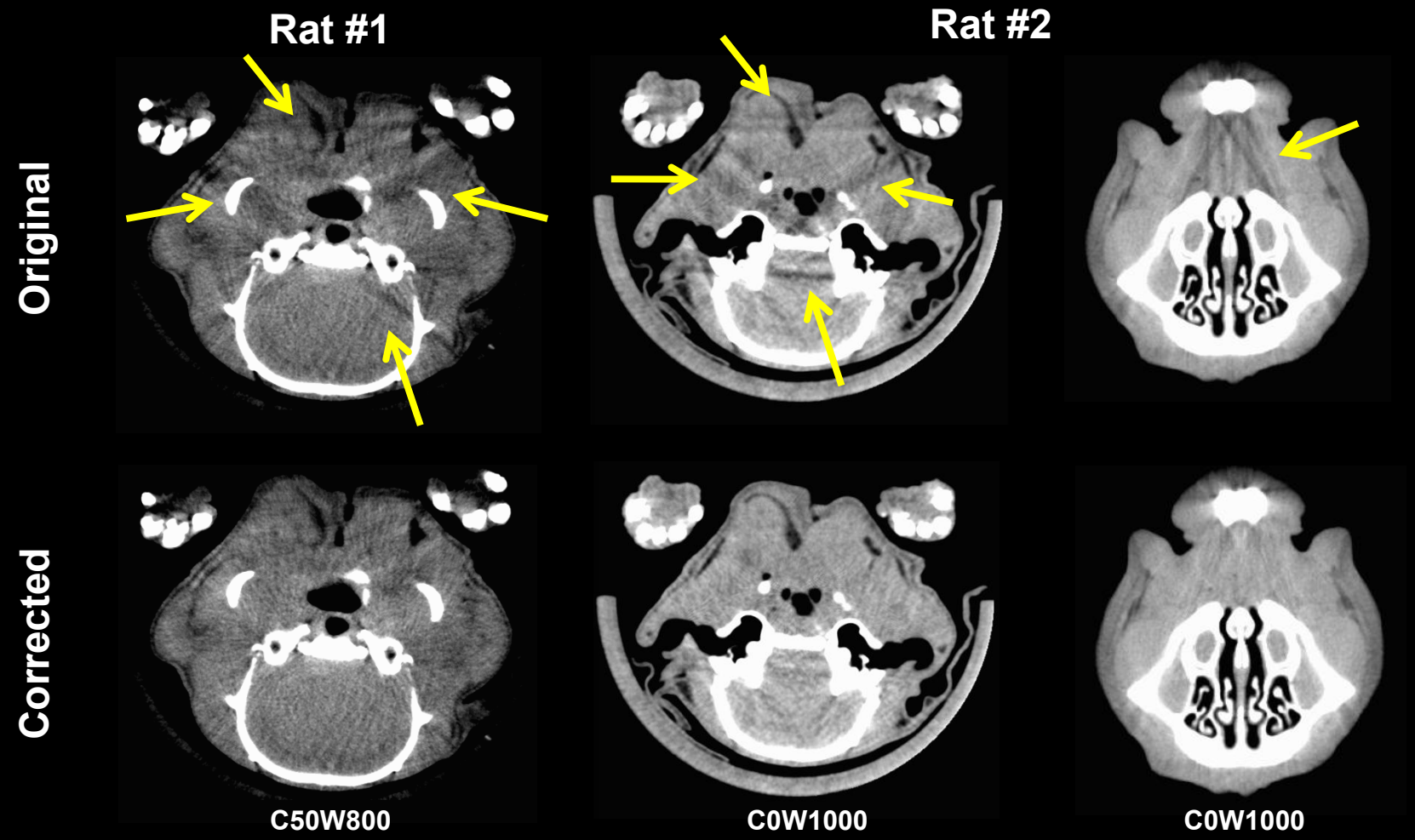

Y. Kyriakou, E. Meyer, D. Prell, and M. Kachelrieß, “Empirical beam hardening correction (EBHC) for CT,” Med. Phys. 37(10):5179-5187, October 2010.

dkfz.

EBHC: Clinical CT vs. FD-CT

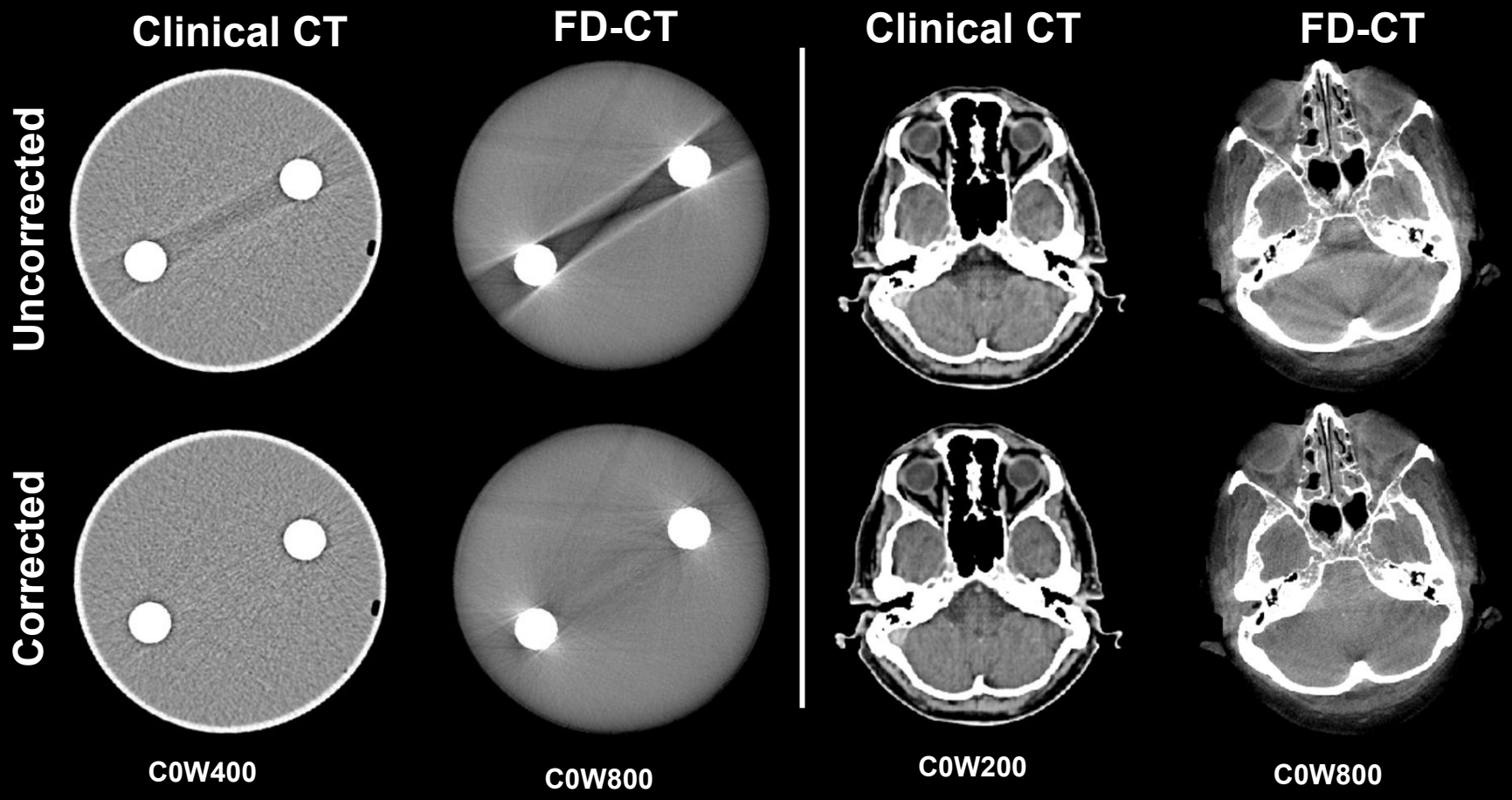

Y. Kyriakou, E. Meyer, D. Prell, and M. Kachelrieß, “Empirical beam hardening correction (EBHC) for CT,” Med. Phys. 37(10):5179-5187, October 2010.

dkfz.

Conclusions on Empirical Cupping and Beam Hardening Corrections

- X-ray spectra need not necessarily be known
- Scatter is implicitly accounted for as well
- ECC and EBHC are robust methods that work well in clinical CT and that also have been applied to some industrial situations.

Further Reading

- Yunsong Zhao, and Mengfei Li. Iterative Beam Hardening Correction for Multi-Material Objects. PLoS ONE 10(12):1-13, December 2015.
- Hyoung Suk Park, Dosik Hwang, and Jin Keun Seo. Metal Artifact Reduction for Polychromatic X-ray CT Based on a Beam-Hardening Corrector. IEEE TMI 35(2):480-487, September 2015.
- Rune Slot Thing, Uffe Bernchou, Ernesto Mainegra-Hing, Olfred Hansen, and Carsten Brink. Hounsfield unit recovery in clinical cone beam CT images of the thorax acquired for image guided radiation therapy. Phys. Med. Biol. 61(15):5781-5802, July 2016.

Linear and non-linear

PARTIAL VOLUME EFFECT

Partial Volume Effect: Experiment

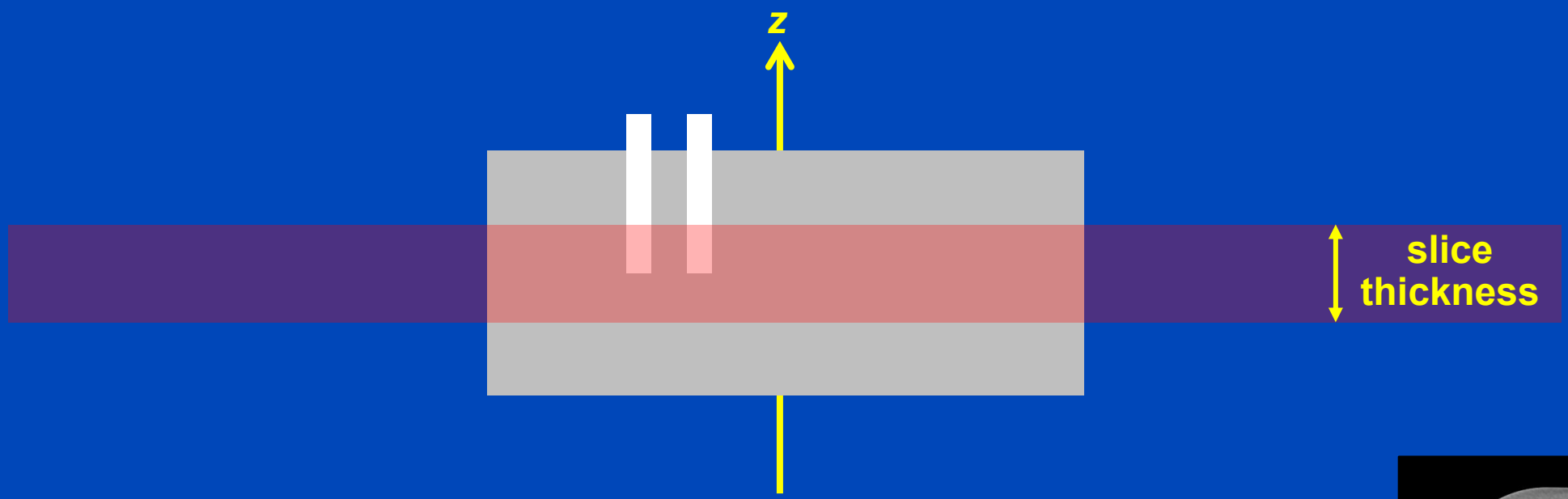

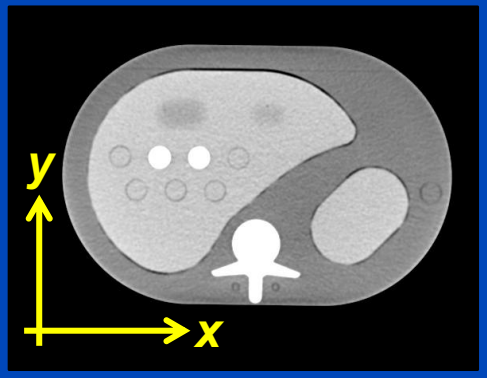

Partial Volume Effect: Experiment

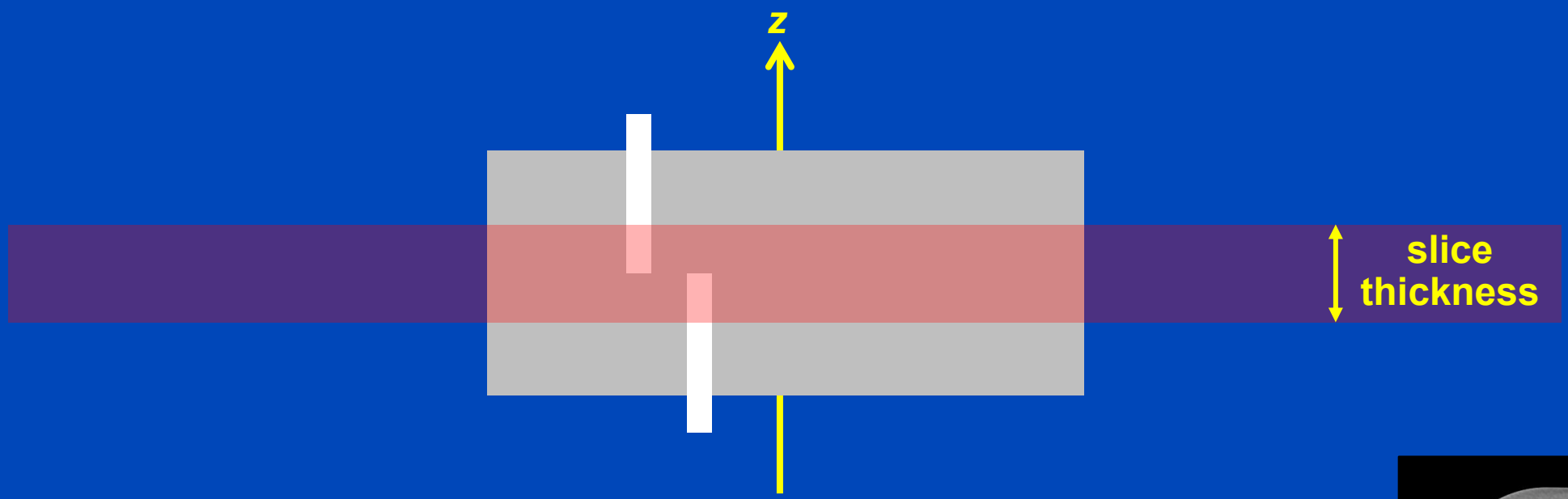

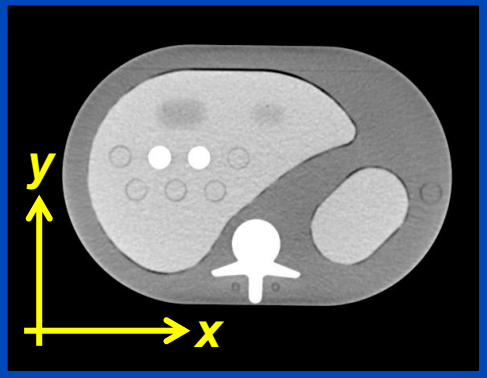

Linear and Non-Linear Partial Volume Effect

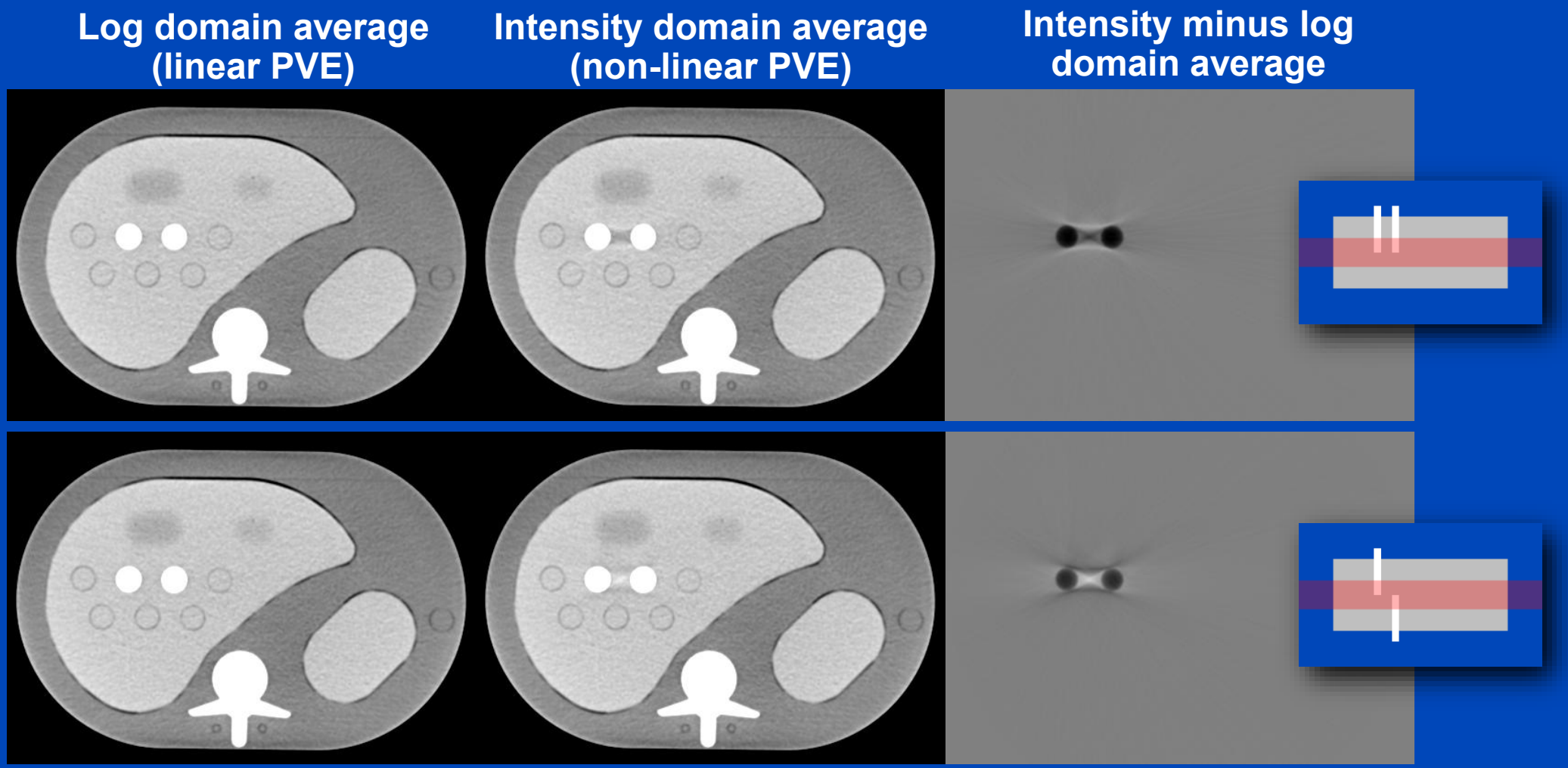

OFF-FOCAL RADIATION

Off-Focal Radiation

- Contribution of off-focal x-rays to the acquired projection data
- Intensities that correspond to high intersection lengths appear too bright
- Underestimation of the component's attenuation

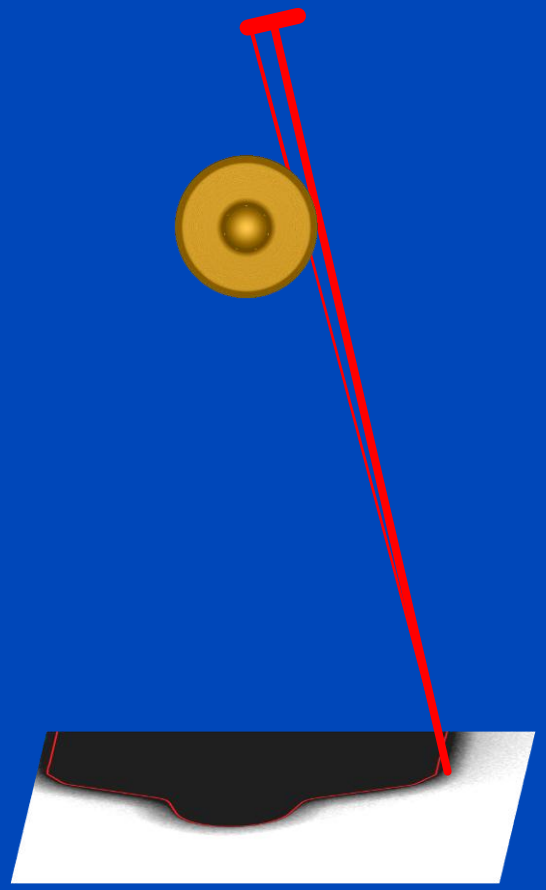

Measured intensities, window level #1

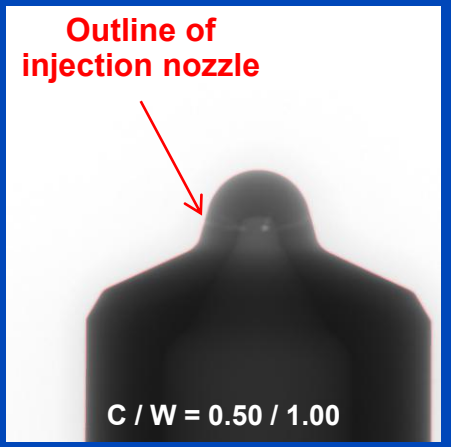

Measured intensities, window level #2

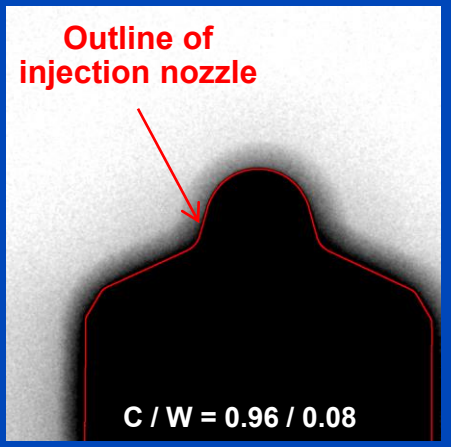

J. Maier, M. Kachelrieß et al. Simulation-based artifact correction (SBAC) for metrological computed tomography. Meas. Sci. Technol. 28(6):065011, May 2017.

dkfz.

Off-Focal Radiation

- Contribution of off-focal x-rays to the acquired projection data
- Intensities that correspond to high intersection lengths appear too bright.
- Underestimation of the component's attenuation

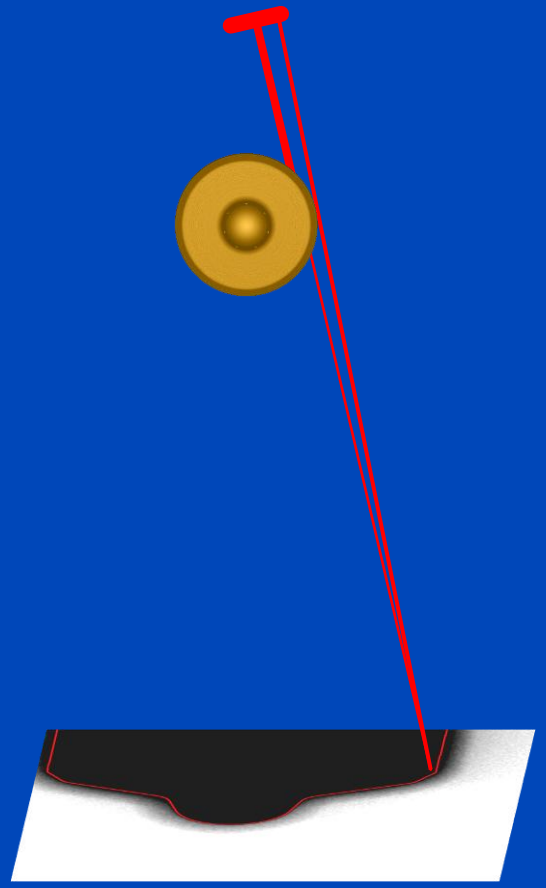

Measured intensities, window level #1

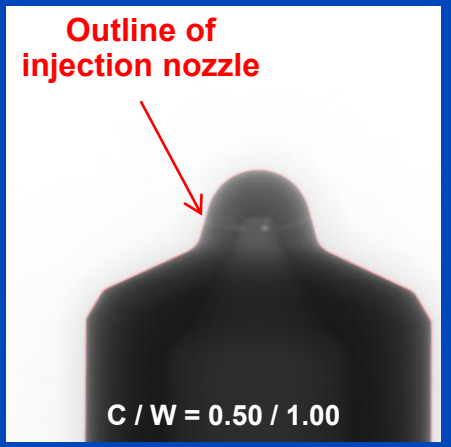

Measured intensities, window level #2

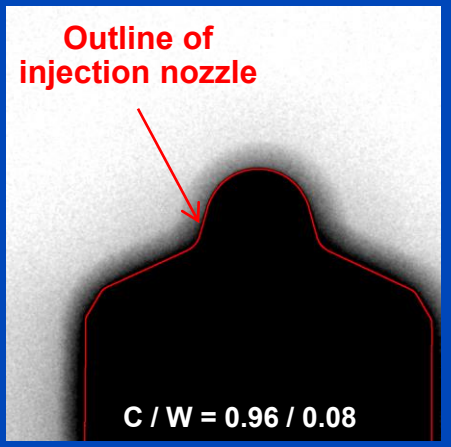

J. Maier, M. Kachelrieß et al. Simulation-based artifact correction (SBAC) for metrological computed tomography. Meas. Sci. Technol. 28(6):065011, May 2017.

dkfz.

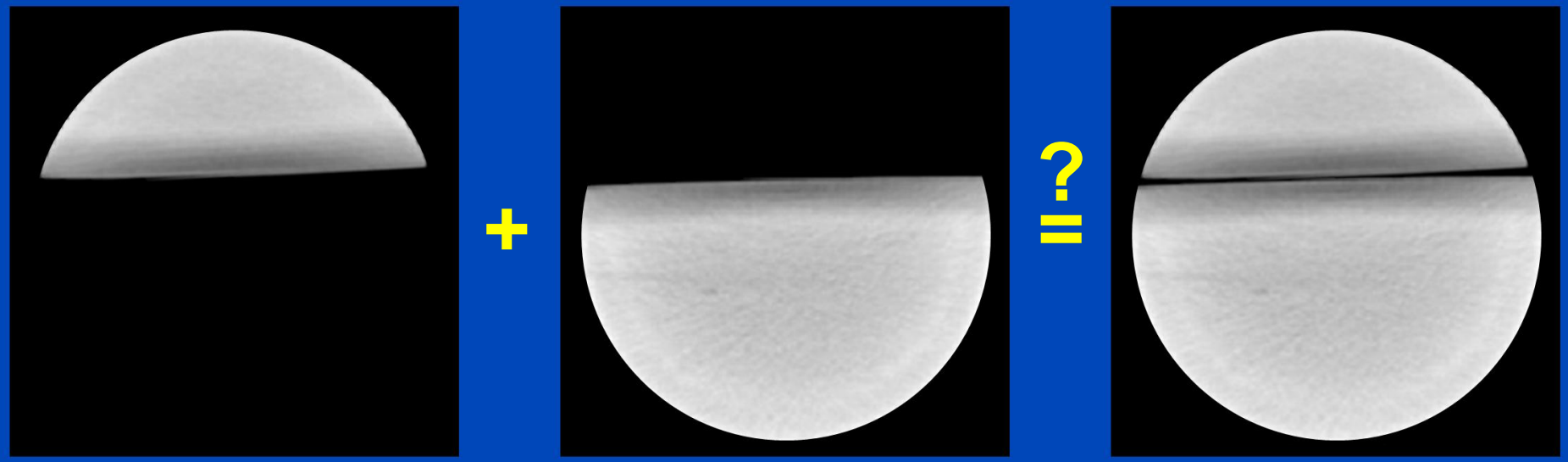

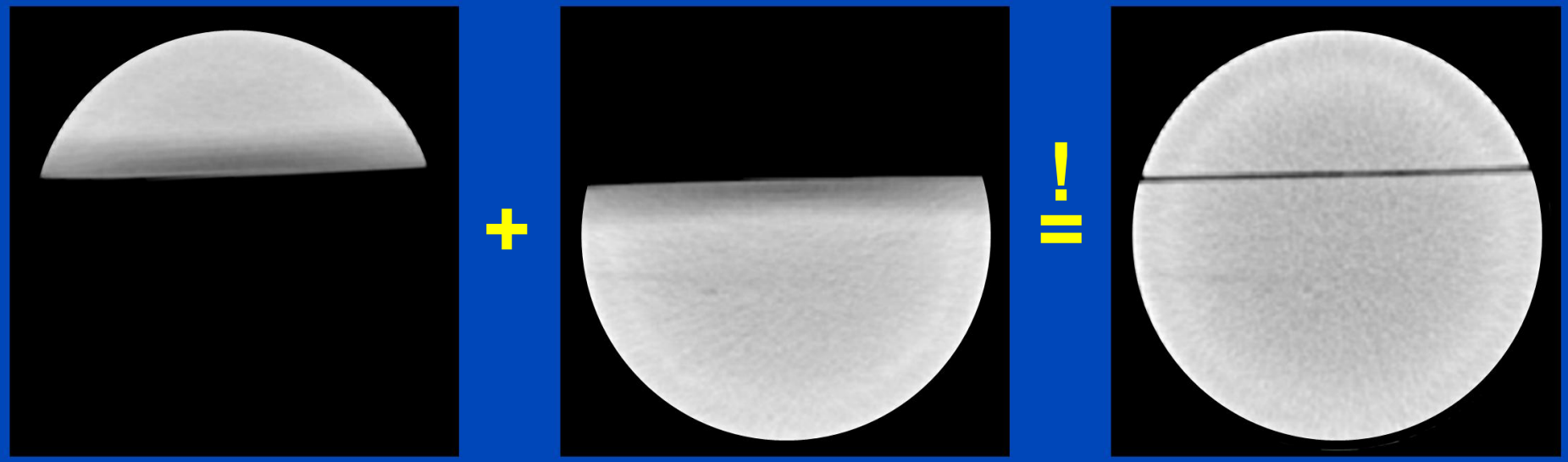

Take Home Messages

- Clinical CT systems use a water precorrection step to minimize cupping artifacts and to normalize to CT units.
- Beam hardening and scatter are a source of typical CT artifacts.
- Several correction methods exist. Some do not need much prior knowledge.

Thank You!

- This presentation will soon be available at www.dkfz.de/ct.
- Job opportunities through DKFZ's international PhD or Postdoctoral Fellowship programs (marc.kachelriess@dkfz.de).
- Parts of the reconstruction software were provided by RayConStruct® GmbH, Nürnberg, Germany.